

Spill it: Measuring oxidative change in oil via  
Fourier transform infrared spectroscopy

Patrick L. Williams  
Helen K. White Ph.D.

Senior Thesis  
May 2, 2014

Haverford College  
370 Lancaster Ave  
Haverford, PA 19041

## Abstract

Since its release into the environment on April 20, 2010, oil from the Deepwater Horizon spill has been extensively studied to assess how it changes in the environment over time. The major factors affecting oil degradation are most likely the presence of light (photooxidation) and the presence of microbes (biodegradation). This study aimed to explore these mechanisms by Fourier-transform infrared spectroscopy (FT-IR) and gas chromatography flame ionization detection spectroscopy (GC-FID). To this end, fresh surrogate oil and previously weathered oil collected from Gulf of Mexico (GoM) coast beaches were incubated with seawater in the presence and absence of sunlight and/or biology. Raw oil was monitored over 21 weeks. Though these weathering analogues were not stringent enough to yield oxidative change on levels seen in environmental samples, FT-IR was able to detect subtle changes in oxygenated functional groups. Oil soaked sand patties were monitored for 42 weeks. OSPs appeared to not weather during the incubation. Combined, these results support the idea that FT-IR, while potentially useful in conjunction with other analytical methods should not be used as the sole preliminary screening tool to test oxidative weathering of marine oil.

## Acknowledgements

The last four years or so have been a tremendous amount of fun. As always I would like to thank Helen White for her support, enthusiasm, and guidance through this past year and for those before. I have grown, traveled, and learned much in my time working with her and I am grateful for all the opportunities she helped me discover and the skills she has imparted. This project has been new for both of us and it has been a delight to have her as a mentor. Her impeccable taste in music has kept me sane in my darkest hours for that I am forever in debt.

I must also thank Jen Reeve for her help in lab and out. We laughed, we cried, and in the end science happened. I also need to thank the other members of the White lab. Alana was indispensable in helping me prep innumerable samples, Max for being the even keel on an otherwise windswept ship, Shelby for her humor (and her sand patties), and the rest of the White lab who have made this year a joy. To all those friends who have put up with my bizarre work hours and endless science library shifts I also owe you thanks. Your numerous distractions from and reminders of the world outside of Science were always appreciated.

The Haverford College Chemistry Department has been an incredible source of strength, knowledge, humor and help these past four years. The opportunities provided and their bona fide sense of community has made my time here a pleasure.

Finally I would like to thank my parents, Ken and Barb, for their love, support, and patience. Mammy and pappy Williams: you have taught me so much–this better go on the fridge.

## Table of contents:

Abstract	2
Acknowledgements	3
Table of contents:	4
Table of figures	5
Introduction	8
The spill, occurrence and distribution of oil	8
Background and composition of raw oil	12
Weathering oil: evaporation, dissolution, photooxidation, biodegradation	14
Persistence of oil including OSPs	18
Instrumental analysis of oil (GC, GCxGC, FTIR)	19
Methods	27
Sample collection	27
Incubation: raw oil	28
Incubation: oil soaked sand patties	29
Sample extraction and preparation	30
FT-IR analysis	31
GC-FID analysis	33
2D correlation analysis	34
Results	35
Raw oil incubation	37
Effects of light and dark systems	39
Effects of biotic and abiotic systems	45
Raw oil incubation summary	51
Oil soaked sand incubation	51
Effects of light and dark systems	54
Effects of biotic and abiotic systems	56
Oil soaked sand incubation summary	57
Discussion	58
Future directions	61
Works cited	63
Appendix:	66
A: Pristane/phytane ratios	66
B: Raw oil incubation extraction data	67
C: Raw oil and OSP FT-IR average integrations	68
D: Raw oil and OSP FT-IR average peak ratios	76

## Table of figures

<b>Figure 1:</b> A map of the total oiled areas as of July 31. Credit: New York Times	8
<b>Figure 2:</b> Data from Ryerson et al. showing compounds and their mass fraction in the atmosphere (A), slick (B), and plume (C) 12 following the DWH spill and a schematic of oil traveling through the water column, surface, and atmosphere (D-values are in millions of kilograms per day).	11
<b>Figure 3:</b> Illustration showing the potential pathways of spilled oil following the 2010 DWH incident in the Gulf.	15
<b>Figure 4:</b> Oil soaked sand patty (OSP) collected from Ship Island, MS in July 2010.	16
<b>Figure 5:</b> Compiled TLC-FID data of oil soaked sands collected in the summer of 2012. Across all patties there are large polar fractions comprising on average 70% of the entire sample (White and Williams unpublished data).	20
<b>Figure 6:</b> Correlations observed within TLC-FID analyses. The Relative percent of FOxy2 versus FSat ( $R^2 = 0.80$ ) as determined by TLC-FID is shown in. All samples were collected in June and July 2012 and symbols that are labeled and filled are those described in Figures 2 and 3 (White and Williams unpublished data).	22
<b>Figure 7:</b> (A) GC-FID, (B) TLC-FID, and (C) FT-IR of oil extracted from (a) WL06 and (b) WL13 rock scrapings and (c) EI14 and (d) EI15, which represent the inside and outside of a large oil-soaked sand patty respectively.	24
<b>Figure 8:</b> Sites of sample collection. PC=Pensacola, FL, FP=Fort Pickens, Pensacola, FL, PD=Perdido Key, FL, GS=Gulf Shores, AL, FM=Fort Morgan, AL, DI=Dauphin Island, AL, PG=Pascagoula, MS, BX=Porter Ave Biloxi, MS, SI= Ship Island, MS, GP=Gulf Port, MS, WL= Waveland Jetty, MS, GI=Grand Isle, LA Public Beach, Grand Isle, LA, EI=Elmer's Island, LA, PF=Port Fourchon, LA).	28

<b>Figure 9:</b>	29
A summary of the various raw oil incubations and simulated environmental perturbations.	
<b>Figure 10:</b>	30
A summary of the various raw oil incubations and simulated environmental perturbations.	
<b>Figure 11:</b>	30
FT-IR spectra showing the areas of interest and the functional groups they represent.	
<b>Figure 11 (cont.):</b>	30
The figure shows the integration scheme for all the peaks with the solid lines outlining the integration areas of selected peaks and the doted line showing the area for the CH total integration.	
<b>Figure 12:</b>	34
2DCA equations (right) where $\phi$ is the synchronous spectrum, $\psi$ is the asynchronous spectrum, $v_1$ and $v_2$ are spectral channels, $y$ is a vector of the signal intensities in column $v$ , $n$ is the number of signals in the original dataset, and $N$ is the Noda-Hilbert transform matrix. The graph (left) shows the synchronous spectra and how to interpret it—where positive correlation across the diagonal represents two peaks growing or shrinking together, and negative correlation indicates one peak growing and the other shrinking at the same time.	
<b>Figure 13:</b>	36
The GC-FID of raw surrogate oil shows characteristic abundance of both low and high molecular weight saturated alkanes, a small UCM, and confirmed pristane/phytane ratios (see appendix A).	
<b>Figure 14:</b>	36
The FT-IR of raw surrogate oil shows an expected lack of peaks corresponding to oxidized functional groups.	
<b>Figure 15:</b>	37
GC-FID chromatogram of raw oil exposed to sunlight for 12 weeks.	
<b>Figure 16:</b>	38
FT-IR spectra of raw oil exposed to light for 21 weeks.	
<b>Figure 17:</b>	40
GC-FID (12 weeks exposure) and FT-IR (21 weeks exposure) of raw oil incubations A (light, abiotic), D (light, biotic), and C (dark, abiotic).	

<b>Figure 17 (cont):</b>	41
FT-IR spectra showing a full spectral view (left) and a zoomed in window to highlight the C=O, C=C, and C-O peaks.	
<b>Figure 18:</b>	43
FT-IR peak heights. X-axis represents weeks incubated.	
<b>Figure 19:</b>	44
Internal ratios of FT-IR integrations exposed to light. X-axis represents weeks incubated.	
<b>Figure 20:</b>	46
GC-FID (12 weeks exposure) and FT-IR (21 weeks exposure) of raw oil incubations B (dark, biotic), D (light, biotic), and C (dark, abiotic).	
<b>Figure 20 (cont):</b>	47
FT-IR spectra showing a full spectral view (left) and a zoomed in window to highlight the C=O, C=C, and C-O peaks.	
<b>Figure 21:</b>	49
FT-IR peak heights. X-axis represents weeks incubated. Once again the peak heights over time of samples exposed to microbes are very stable. Peak integrations need to be used to test a broader range of functional group environments.	
<b>Figure 22:</b>	50
Internal ratios of FT-IR integrations. X-axis represents weeks incubated.	
<b>Figure 23:</b>	52
GC-FID plots of the two OSPs used in the incubation.	
<b>Figure 24:</b>	53
Initial FT-IR spectra of the two OSPs used in the incubation.	
<b>Figure 25:</b>	54
Internal ratios of FT-IR integrations. (T3=21 weeks of exposure and T6=42 weeks exposure).	
<b>Figure 26:</b>	56
Internal ratios of FT-IR integrations. (T3=21 weeks of exposure and T6=42 weeks exposure).	

## Introduction

### The spill, occurrence and distribution of oil

On April 20, 2010 the Deepwater Horizon (DWH) semi-submersible mobile offshore drilling unit exploded about 40 miles off the Louisiana coast at a depth of 1500 meters. The Macondo wellhead was uncovered for 87 days, and was finally capped on July 15th. The spill released 4.9 million barrels of oil into the Gulf of Mexico (GoM).<sup>1</sup> Figure 1 shows the extent of effected waters and beaches and the intensity of oiling along the GoM coast. The spill affected almost 180,000 km<sup>2</sup> of open water as well as over 1,600 km of shoreline. Cleanup crews during and after the spill employed many different techniques to collect, disperse, or consume the oil, ranging from physical removal with skimmers to chemical dissolution into the water column. While a small fraction of oil was corralled and scooped out of the Gulf, most of it was burned or chemically dispersed.

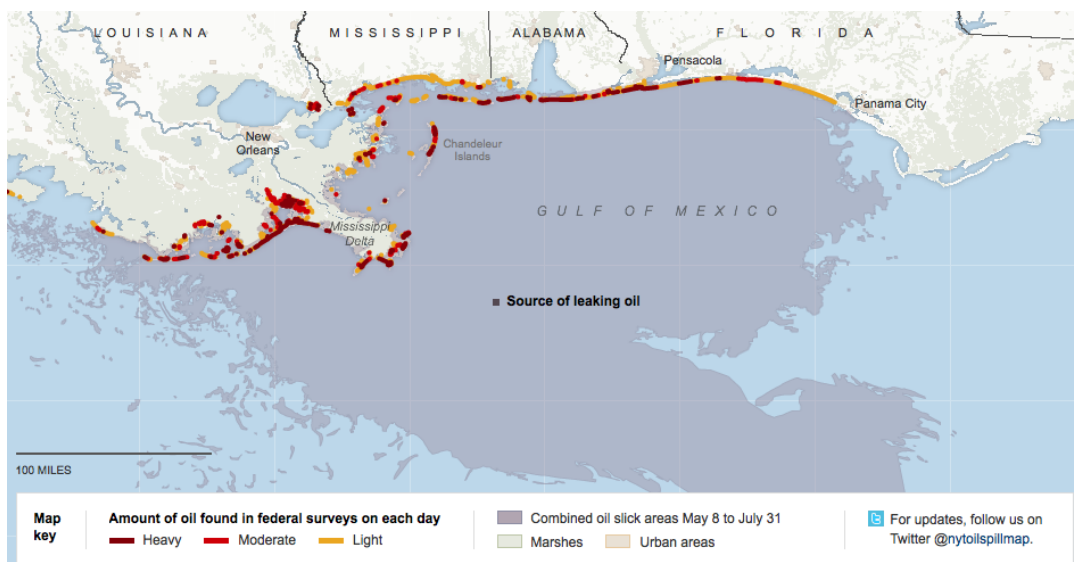


Figure 1: A map of the total oiled areas as of July 31. Credit: New York Times

Because the DWH spill is one of the largest US spills to date, it presents a unique opportunity to study the fate of oil in the marine environment. The quantity of oil spilled, coupled with the fact that oil was released at depth, presented a notable opportunity for scientific study. The large area affected by the spill also means that the oil can be examined across large spatial scales. There will obviously be long term environmental impacts, but because scientific understanding of weathering, migratory, and biological incorporation of oil is not well developed, these affects will need to be monitored closely.

The federal government's Operational Science and Advisory Team (OSAT) published a report in December 2010 stating that at the time of publication there was no "actionable" oil in water or gulf shores—meaning that oil had either been cleaned or dispersed enough that large scale clean up efforts were no longer effective.<sup>2</sup> This meant that whatever oil was still in the GoM was effectively there to stay. It thus became imperative that this environmental oil be understood on a chemical, biological, and ecosystem-wide level.

Initial studies focused on measuring the quantities, composition, and movement of oil from depth to the surface and through the water column and atmosphere. Flow experiments were conducted at the wellhead to determine how much crude oil was released into the Gulf.<sup>1</sup> Reddy et al. determined that the DWH well was leaking at a rate of about  $85 \pm 15 \text{ kg s}^{-1}$ , or  $57,000 \pm 9,800$  barrels of oil per day. This was in conjunction with  $24 \pm 4.2 \text{ kg s}^{-1}$  of natural gas (methane through pentanes), meaning  $110 \pm 19 \text{ kg s}^{-1}$  of hydrocarbons was being released into the gulf over 87 days. Other studies focused on changes in marine populations. Whitehead et al. explored the effect of oil on marsh

fishes, measuring oil exposure and linking changes in genome expression and biological response to degrees of exposure.<sup>3</sup> Other groups focused on tracking and quantifying oil and dispersants through the water column. Kujawinski et al. were able to find DOSS (a dispersant) where the EPA had failed after developing an extraction method 1,000 times more sensitive than the industry standard.<sup>4</sup> Nearly 800 peer-reviewed publications and technical reports have been published to date specifically dealing with the DWH spill.<sup>5</sup> Because of the strength in the scientific community's initial response, the early stages of the DWH spill have been well documented. However, oil is not chemically stable in the environment and as such developing an understanding of how oil changes over extended periods of time is a critical step in determining the fate of marine oil. Ryerson et al. performed an exhaustive series of airborne, surface, and subsurface measurements during May and June of the spill to establish the fate of oil coming from the blowout. They discovered that only 25% (by mass) of DWH oil was water soluble, but 69% (by mass) of the plume coming from the wellhead was made up of these soluble hydrocarbons—mainly methane ( $\text{CH}_4$ ), ethane ( $\text{C}_2\text{H}_6$ ), propane ( $\text{C}_3\text{H}_8$ ), and isomers of butane ( $\text{C}_4\text{H}_{10}$ ). The other 31% of the plume was comprised of small droplets of insoluble products that made their way to the surface to evaporate or form slicks. Of this 31%, ~16% evaporated, ~30% formed a slick, and the rest slowly dispersed into the water column as it rose. Figure 2 shows a summary of mass fractions of compounds found in the plume, slick, and atmosphere, as well as a schematic showing the fate of DWH oil.<sup>6</sup> It should be noted that in the Figure ~23% of the released oil is unaccounted for. It is likely that this oil was deposited on the sea floor.<sup>6</sup>

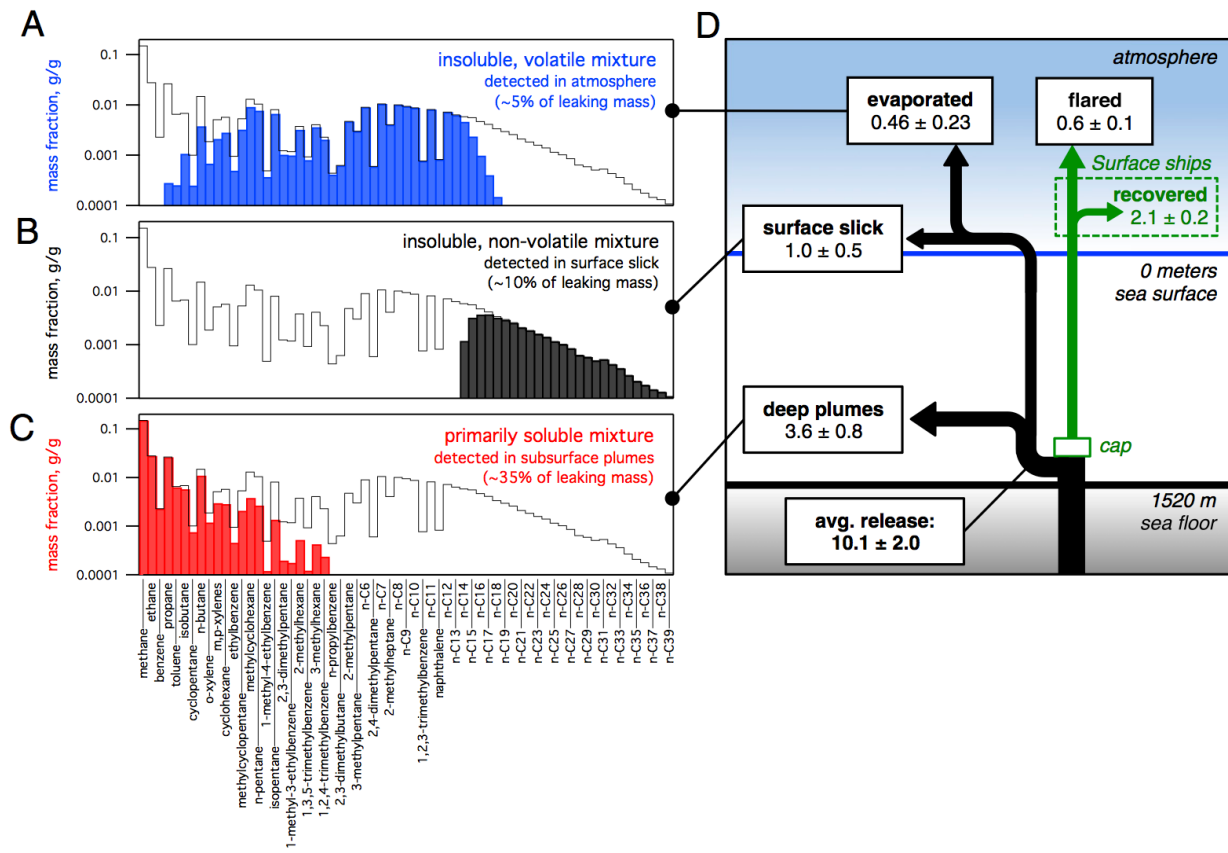


Figure 2: Data from Ryerson et al. showing compounds and their mass fraction in the atmosphere (A), slick (B), and plume (C) following the DWH spill and a schematic of oil traveling through the water column, surface, and atmosphere (D—values are in millions of kilograms per day).

By December 17, 2010 OSAT estimated that only about one quarter of released oil was recovered by clean-up response teams. About 5% was burned, 3% was skimmed, and 17% recovered via the riser pipe from the DWH rig. The rest dissolved, evaporated, or washed ashore.<sup>7</sup> In the end, while significant quantities of oil were collected or treated, an estimated 22% (over 1 million gallons) remains in the Gulf or coastal areas.<sup>8</sup> The sheer magnitude and variety of the issues caused by the Macondo spill requires a multi-faceted research approach where scientists of all backgrounds can come together to better understand the impact of this event.

## **Background and composition of raw oil**

Oil is formed from buried organic matter than has been subjected to extreme heat and pressure over millions of years. Oil is comprised predominantly of hydrocarbons, but also contains hydrocarbons bound or complexed with heteroatoms and metals such as nickel, lead, vanadium, cadmium, and iron.<sup>9</sup> Macondo oil was "sweet crude oil," meaning it contained very little sulfur, but other heteroatoms can also be present (oxygen and nitrogen specifically). Macondo oil is comprised of less than 0.5% nitrogen and sulfur. The rest is mostly carbon (86.6%) and hydrogen (12.6%).<sup>1</sup>

There are hundreds of specific chemical compounds that make up crude oil, but most are characterized based on their chemical and structural properties. Paraffins are straight or branched carbon chains taking the form  $C_nH_{2n+2}$ , the smallest being methane and the largest around n=28 to 35. Aromatics are mostly benzene derivatives (compounds with cyclic pi systems) or polycyclic aromatic hydrocarbons (PAHs). Cycloalkanes, alkenes, dienes, and alkynes are also present in smaller quantities. Biomarkers are compounds that usually fall into the above categories with the added caveat that they resist degradation. These are present in specific ratios which vary from wellhead to wellhead and can be used to establish points of origin for oil. Hopanes (found in eukaryotes) and steranes (found in prokaryotes) are pentacyclic compounds involved in strengthening and maintaining rigidity of cell membranes and are often used as biomarkers. The hopane/sterane ratio is highly specific to the wellhead. It was necessary to establish Mocando biomarkers early on in the research process so the oil could be tracked effectively. Using biomarkers, labs were able to prove how far DWH oil traveled and how it was affecting GoM plant, animal, and human communities. White et

al. were able to prove that DWH oil was responsible for coral deaths in deep water.<sup>10</sup> Reddy et al. used these biomarkers to track the changing composition and location of DWH oil around the northern gulf.<sup>11</sup> As part of any study trying to link DWH oil to environmental responses, it is necessary to analyze these biomarkers and link them to the source oil.

Most compounds in oil identified to date are non-polar saturated or unsaturated hydrocarbons. While these make up the bulk of oil, there remain polar and water soluble fractions that are not well understood. About 15% of the compounds by mass in DWH oil contain oxygen. However, nearly 60% of the the water soluble fraction (the most mobile fraction) of oil contains oxygenated compounds.<sup>12</sup> These molecules are difficult to isolate via traditional methods that rely on non-polar organic solvents and silica columns where the polar compounds cannot elute off onto a detector (GC-MS and GC-FID). Toxicology studies continue to explore the affects all fractions of oil have on plant and animal populations in the GoM. However, most of these studies either use exposure to raw oil or simply monitor changes in communities of fish, corals, or other abundant marine populations. Scarlett et al. worked with aromatic and non-aromatic naphthenic acids—a class of polar carboxylic acids with a carbon backbone of 9 to 20 carbons. They were able to prove that these compounds were toxic to larval zebrafish at LC50 values around 8mg/L.<sup>13</sup> In the past Wolfe et al. were able to prove that polar oil fractions were as toxic as aromatic fractions—an important result as PAHs are usually thought to be some of the most dangerous compounds found in oil.<sup>14</sup> Paterson et al. studied long term exposure of weathered oil after the Exxon Valdez spill and established that this more polar oil was still having negative effects on wildlife. This included studies of

sediment-affiliated species like fish, otters, and ducks.<sup>15</sup> Polar fractions of oil have been documented to be both extremely recalcitrant and potentially dangerous to GoM communities. It is thus essential that scientists fully understand this portion of oil.

### **Weathering oil: evaporation, dissolution, photooxidation, biodegradation**

Understanding oil degradation and changes over time is important in the context of the DWH spill because a significant quantity remains in the environment. Oil has been found in sediments at depth and along the coast, as oil-soaked sand patties (OSPs), as well as trapped beneath the sunken DWH rig.<sup>16,17</sup> In these environments, oil continues to be exposed to chemical, biological, and mechanical forms of weathering. Because this oil will be affecting ocean and coastal communities for years, it is necessary to understand its chemical properties.

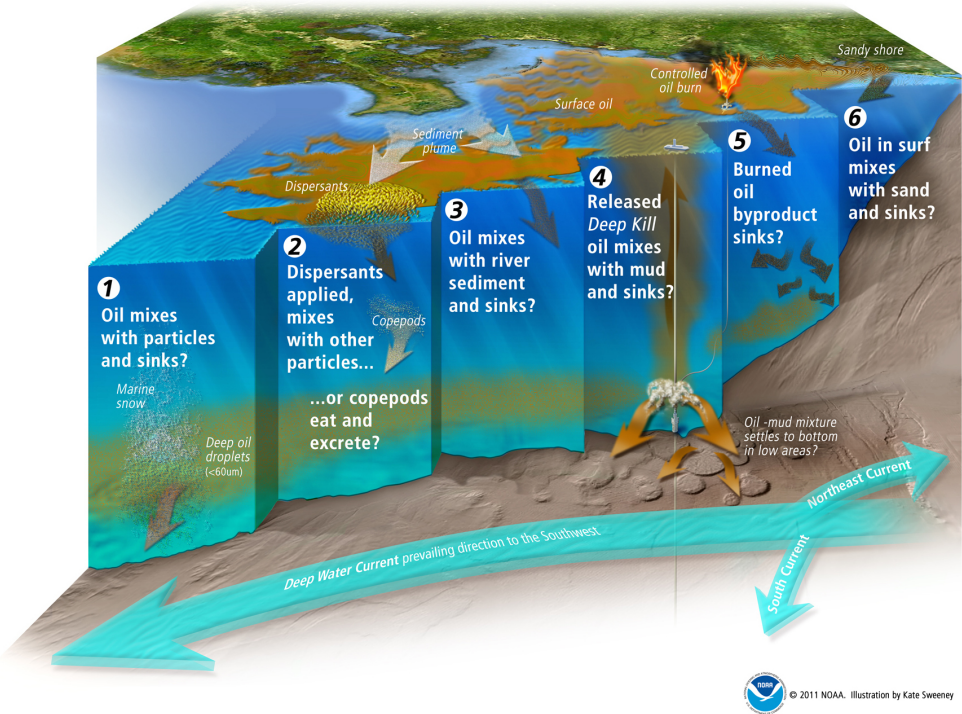


Figure 3: Illustration showing the potential pathways of spilled oil following the 2010 DWH incident in the Gulf.<sup>18</sup>

Figure 3 summarizes the mobility as well as the potential fate of DWH water following the spill. When released from the wellhead, oil mixes with water, allowing for dissolution of volatile compounds throughout the water column before reaching the surface. Samples taken a little above the wellhead contained about 5% water (vol/vol), while samples taken a few meters up the plume contained 23% water due to turbulent mixing.<sup>11</sup> Upon reaching the surface some compounds evaporate and others form a surface slick. Some slicks were churned by waves and wind to form emulsions. The oil, carried by currents, spread and eventually reached beaches from Texas to Florida. Some oil sank back down to the ocean floor to form large mats. These can then break up and wash to shore. Figure 4 shows a product of these mats; an amalgam of sand,

oil, and other organic matter that has been washing up in chunks since the spill and continue to do so (as of January 2014).

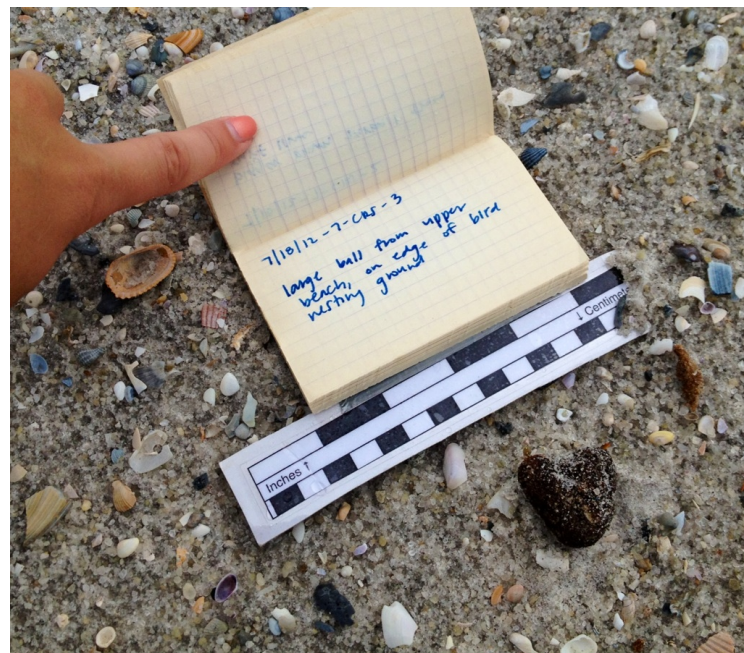


Figure 4: Oil soaked sand patty (OSP) collected from Ship Island, MS in July 2010.

The simplest means of oil weathering have already been mentioned—dissolution and evaporation. Volatile compounds disperse while more recalcitrant hydrophobic hydrocarbons persist. As part of the cleanup effort following the DWH spill, dispersants were applied and some slicks were burned. Dispersants make oil form small droplets that may be more available to bacterial endocytosis. Burning oil creates various byproducts that can also be found in environmental samples. Weathering of oil due to evaporation and dissolution had been well documented before the DWH spill. Straight-chain alkanes and aromatic compounds are almost completely degraded and oxidized when exposed to light and microbial degradation. Maki et al. documented 70% and 40% reductions in saturated and aromatic fractions respectively upon photooxidation and

biodegradation. Their work also showed that oil exposed to seawater and UV light caused a further decrease in aromatic compounds, coupled with a concomitant increase in resin and asphaltene compounds. This irradiation also decreased the average molecular weight of compounds and an enrichment in oxygen (using field desorption–mass spectrometric analysis). Maki et al. also showed that these oxidized irradiated samples were more bioavailable food sources for microbes.<sup>19</sup> In terms of DWH oil research, studies have shown that short chain n-alkanes (C<sub>1</sub>-C<sub>15</sub>) were lost in the first few weeks after the spill.<sup>20</sup> Methane and other volatile compounds (ethane, benzene, and C<sub>3</sub>-C<sub>6</sub> alkanes) were almost completely dissolved into the water column below 800 m—a unique characteristic of a spill at depth as opposed to a “classic” surface spill.<sup>21,22</sup> C<sub>2</sub> through C<sub>11</sub> hydrocarbons were found in Gulf air samples above the spill, as were measurable quantities of carbon dioxide, monoxide, aromatic compounds, and black carbon from the plume and surface burning byproducts.<sup>23</sup>

Increased levels of oxygenated functional groups within oil samples such as carboxylic acids, esters, and carbonyls were documented by Aeppli et al. They were able to prove that exposing DWH oil to light and seawater usually results in an increase in weight of about 1.5% as oxygen is incorporated into hydrocarbon backbones. Oxidation of alkanes and alkenes, oxidative cleavage, and addition of alkyl side chains to aromatic compounds have all been documented in DWH oil.<sup>24,25</sup> Thus as oil degrades it becomes more polar. This chemical change is important for a few reasons. As polarity increases, the products may become more soluble, further contaminating the water column over time. Polar functional groups mean more opportunities for coordination with metals, which in turn can generate radicals in conjunction with pi systems of aromatic

compounds.<sup>26</sup> These reactive compounds can disrupt any number of metabolic pathways. More polar compounds may also be more bioavailable as they can cross lipid bilayers. Thus weathered (oxidized) byproducts of oil could interfere with biological pathways than their non-polar non-weathered counterparts. In environmental samples evidence of all these forms of oil weathering are present.

Dutta and Harayama have shown that biodegradation preferentially selects for n-alkanes > naphthalenes > branched alkanes > fluorenes > phenanthrenes > dibenzothiophenes. Many organisms synthesize proteins that can degrade hydrocarbons. These microbes have been found across many Gulf oil and sediment samples. Because Macondo oil is a light crude oil (made of lower molecular weight hydrocarbons) much of the oil is readily available for ingestion by bacteria.<sup>27</sup> Past bioremediation studies by Atlas and Hazen using Exxon Valdez oil show that under the right conditions bacteria can remove up to 1.2% of oil by mass from the environment at the beginning of a spill. There was evidence of bacterial activity in the plume of oil erupting from the wellhead and degrading mostly short chain alkanes. There was very little microbial activity on surface slicks, but as the oil washed ashore, near-shore and terrestrial bacteria once again became important degradation factors.<sup>28</sup>

### **Persistence of oil including OSPs**

The oil that did not evaporate, dissolve, or was physically removed endures in coastal waters of the GoM as large oil mats. These break up and the resultant oil-soaked sand patties (OSPs) wash ashore. These are small aggregations of about 20% oil by mass mixed with sand, shells, and other organic matter. As of January 2014 these

OSPs were still being deposited on GoM beaches. Four years after the spill beaches are still being oiled.<sup>29</sup> Plant et al. published a summary of modeled scenarios to track the formation and movement of OSPs in the GoM. Combining surface, current, and sediment data they were able to model the oiling of beaches to both predict sites in need of cleanup response and identify sites that could be useful to study. Plant et al. showed that OSPs, under non-storm conditions, do not travel along beaches. However, under storm conditions, OSPs become highly mobile. These findings suggest that OSPs are likely to become buried and then unearthed in moments of turbulence, lengthening the time OSPs take to reach shore. This also means that OSPs will persist in sediment and continue to oil beaches for years.<sup>29</sup> Because oil changes as it is affected by various environmental factors (light, temperature, microbes, physical motion etc.) it is vital that the chemical evolution of these OSPs is well documented and understood.

### **Instrumental analysis of oil (GC, GCxGC, FTIR)**

Oil can be separated into fractions based on polarity. The most polar fractions of oil contain about 13% oxygen by mass but remain mostly insoluble in water. It has also been verified that these oxygenated compounds are newly formed over time, not simply preferentially enriched as other compounds degrade.<sup>25</sup> Using advanced gas chromatography techniques and correlation analysis, it has been determined that most oxygenated compounds originate from the saturated fraction of oil—a surprising result as it was originally thought that the more recalcitrant saturates were too stable to be oxidized to the levels seen in older samples. This fraction ( $F_{sat}$  in figure 5) includes alkylcyclopentanes, alkyl cyclohexanes, alkylated bicyclic saturated compounds,

tricyclic terpanoids, alkylbenzenes and C19–C26 sterane and diasterane derived components.<sup>30</sup>

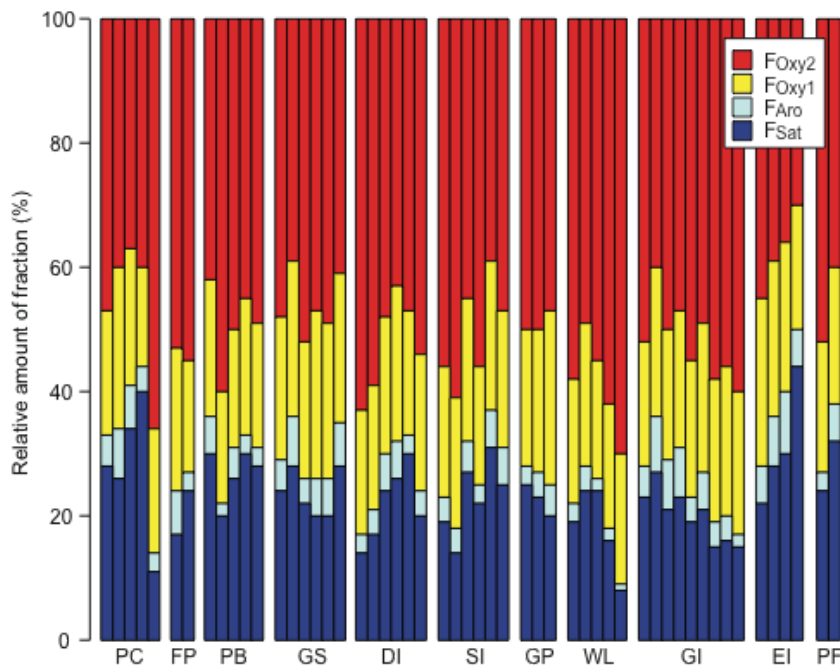


Figure 5: Compiled TLC-FID data of oil soaked sands collected in the summer of 2012. Across all patties there are large polar fractions comprising on average 70% of the entire sample (White and Williams unpublished data). Shown are four fractions of oil: saturated (FSat), aromatic (FAro), and oxygenated (FOxy1 and FOxy2)

Existing research has tried to examine more closely these chemical changes in oil. The industry standard of oil investigation is gas chromatography coupled to a flame ionization detector (GC-FID) and gas chromatography mass spectroscopy (GC-MS). While gas chromatography works with non-polar compounds, as oil weathers and becomes more polar, less and less oil actually makes it through the column and onto the detector. With highly weathered samples, about 20% of the original sample is actually seen on the final chromatogram. As oil degrades a larger unresolved complex mixture (UCM) also develops, further complicating spectral analysis. A UCM is a hump

in a chromatogram that the GC cannot resolve into individual peaks, representing an unknown number of co-eluting products. A different technique is necessary to explore the evolving polar weathering processes of crude oil.

GCxGC-MS (two tandem gas chromatographs and a mass spectrometer) have been used to deconstruct the UCM of a normal gas chromatogram coupled to a mass spectrometer (GC-MS). While this is helpful in exploring the fraction of oil that elutes off the column, the problem remains that only a small fraction of oil is actually being detected when dealing with weathered oil. Running a tandem GC is also time consuming, expensive, and complicated. It is useful, but unfeasible to be used as a primary screening method at this time because it requires such specific training to maintain and use effectively.

Of specific interest in weathering oil are changes in polarity because weathered oil usually means oxygenated oil. Thin layer chromatography coupled to a flame ionization detector (TLC-FID) uses the simple mechanics of a TLC plate combined with a flame detector to measure compounds with different polarities. TLC can be used to measure bulk changes in polarity quickly and with specificity. Figure 5 shows a reduction of this data, indicating the large polar fractions of oil. Shown are four fractions of oil: saturated ( $F_{\text{Sat}}$ ), aromatic ( $F_{\text{Aro}}$ ), and oxygenated ( $F_{\text{Oxy}1}$  and  $F_{\text{Oxy}2}$ ) determined by TLC-FID. The bulk of the samples show large oxygenated fractions and small aromatic and saturated fractions. Figure 6 shows the correlation between increasing polar fractions, and decreasing saturated fractions in environmental OSP samples. Aepli et al have seen similar relationships between oxygenated and non-oxygenated fractions as

well.<sup>17</sup> This data shows that internal changes are happening in DWH oil, rather than addition of other compounds from non-petroleum sources.

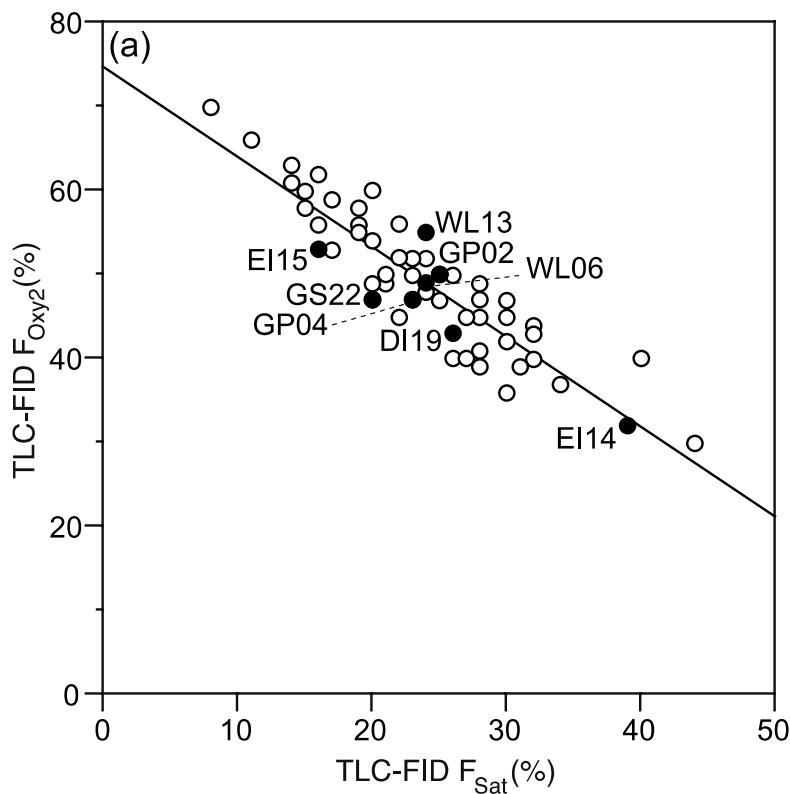


Figure 6: Correlations observed within TLC-FID analyses. The Relative percent of  $F_{\text{Oxy}_2}$  versus  $F_{\text{Sat}}$  ( $R^2 = 0.80$ ) as determined by TLC-FID is shown in. All samples were collected in June and July 2012 and symbols that are labeled and filled are those described in Figures 2 and 3 (White and Williams unpublished data).

While some techniques are proving to be useful in detecting the polar fractions of weathered oil, a satisfactory screening method has yet to be developed. Most methods currently in use are time consuming and expensive. What is needed now is a simple, cheap, and easily standardized method of detecting changes in oxygenation across samples. Infrared spectroscopy meets the necessary qualifications as a screening method for oxidized samples. FT-IR is an easy instrument to use and is ubiquitous in

the field of chemistry. It can also sense oxygenated functional groups with reasonable specificity.

Previous work in the White lab has focused on using IR in conjunction with GC-FID and TLC-FID in an attempt to quantify levels of oxidation in Gulf samples. To date it has been demonstrated that IR can show variations of oxidation levels in OSPs across the Gulf. Most OSPs show plateaued levels of oxidation with about 70% polar fractions in most samples. Figure 7 shows a relationship between GC-FID and TLC-FID chromatograms, and FT-IR spectra. Visually it would appear that there is some correlation between weathered samples and levels of oxidation. The GC-FID chromatograms showing depletion of n-alkanes are also the samples with the largest oxidized peaks in the IR. They also have the largest  $F_{Oxy1}$  and  $F_{Oxy2}$  peaks in the GC-FID chromatograms. This study's goal is to definitively test if FT-IR can detect changing levels of oxidation quantitatively over time to see if IR is a worthwhile screening method for environmental oil.

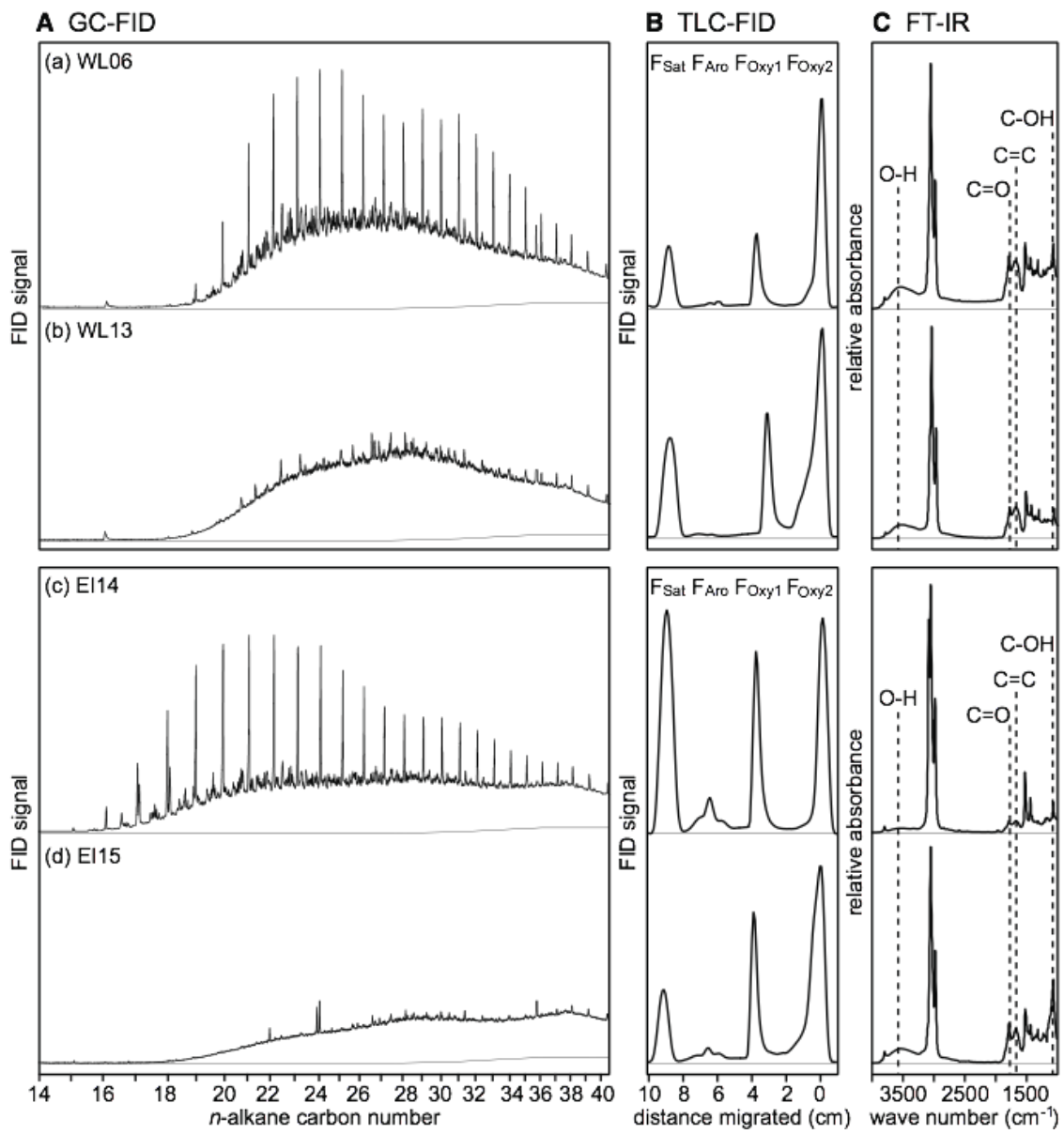


Figure 7: (A) GC-FID, (B) TLC-FID, and (C) FT-IR of oil extracted from (a) WL06 and (b) WL13 rock scrapings and (c) EI14 and (d) EI15, which represent the inside and outside of a large oil-soaked sand patty respectively (Williams and White unpublished data).

Other studies have focused on actively monitoring changes in oil over time. Lab-based incubations have yielded helpful results in elucidating how oil undergoes chemical changes over time. Samples have been irradiated with UV light to explore the

phooxidation-induced changes in various oil samples. The result was a clear decline in aromatic fraction of oil and an increase in polar fractions. This makes sense, as aromatic compounds with their conjugated pi systems are most optically active. It is hypothesized that aromatic compounds could be reacting either by oxidative cleavage of the aromatic rings or by the introduction of oxygenated groups such as hydroxyl or carbonyl to form more polar compounds after exposure to light. There have also been documentation of degradation of biomarkers that were previously thought to be immune to degradation.<sup>31</sup> Radović et al. irradiated raw oil for 12 hours with a  $\text{NrB}_4$  Xe lamp and were able to produce results similar to moderate field conditions. They were able to observe the transformation of saturate and aromatic fractions to more polar, oxygen-containing species.<sup>31</sup> Charrié-Duhaut et al. exposed thin layers of various crude oils to direct summer sunlight for 14 days and were able to measure oxidative changes as well. Their procedure called for extensive extractions and fractionations as well as working at concentrations much higher than this study, but they were able to measure weathering via FT-IR among other techniques.<sup>24</sup>

We hope to use FT-IR in conjunction with GC-FID to explore oil degradation processes over time. Using raw oil and weathered OSPs will give clear pictures of past degradation activities as well as potential future oxidative mechanisms. Using perturbation-based 2D spectroscopy, relationships between peaks can be tracked using external perturbation variable (time, pH, temperature, concentration). The result is a 3D plot (often reduced to a contour plot for easy viewing) that can show if peaks are growing or shrinking together, against one-another, or before/after each other. 2D correlation analysis (2DCA) can offer a unique insight into the environmental processes

associated with oil degradation by showing how oil degrades and the order in which functional groups change. We hope to document substantive changes in oil that undergoes photooxidation and bio-degradation and show that while GC-FID is a useful screening tool for generic oil, FT-IR will provide additional information regarding the oxidation of more weathered samples. While this study will try and use FT-IR by itself as an analytical tool, using it concurrently with other methods is also an option that should not be ruled out.

## Methods

All glassware was combusted at 450°C for eight hours to remove any trace hydrocarbons or washed three times with methanol, dichloromethane, and hexane before use. Other metal tools were also rinsed in the same solvent system. All solvents were spectroscopic grade rated for high-resolution gas chromatography suitable for organic residue analysis (99.9% pure) from Fischer Scientific. No plastics came into contact with samples. Purified air was used to dry tools after solvent rinsing.

## **Sample collection**

Oil soaked sand patties were collected using pre-combusted glass jars, tweezers, and razor blades. Rock scrapings were collected in pre-combusted jars using spatulas. Samples were kept in the dark at ambient temperature until extraction. Figure 8 shows a map of sample sites visited in the summers of 2012 and 2013.

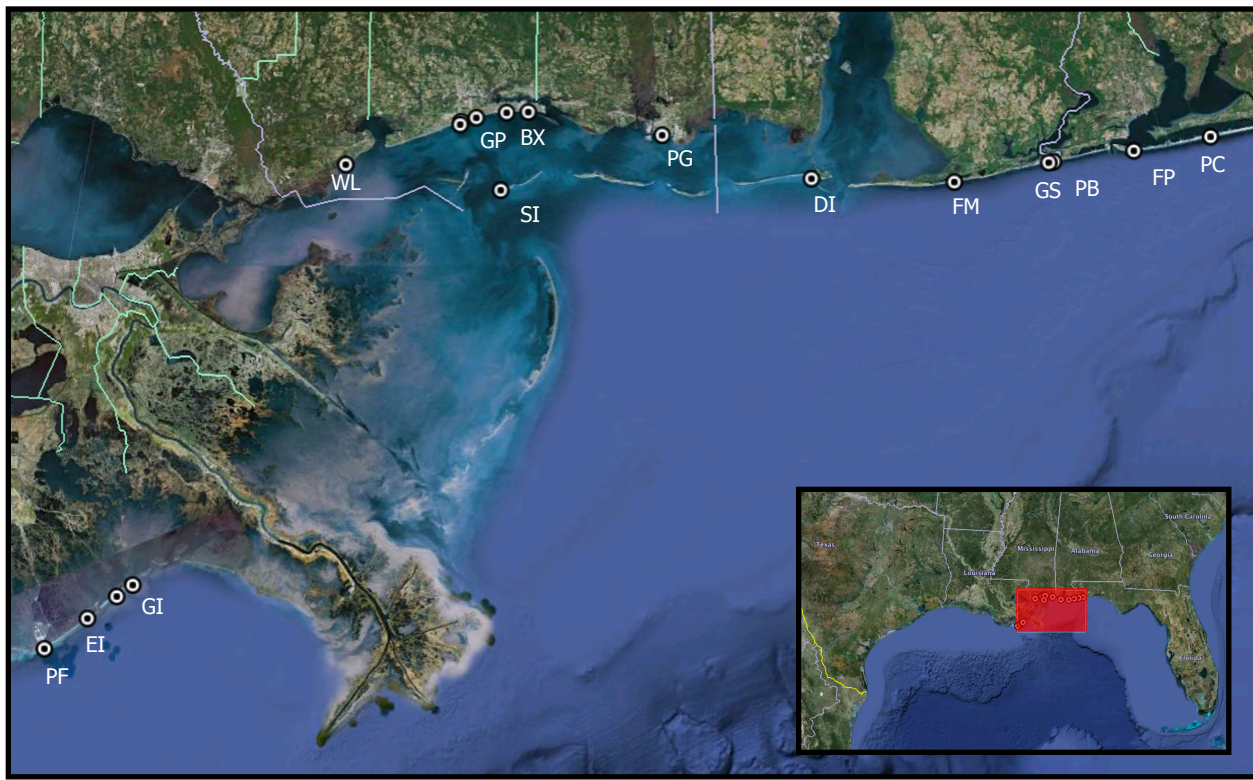
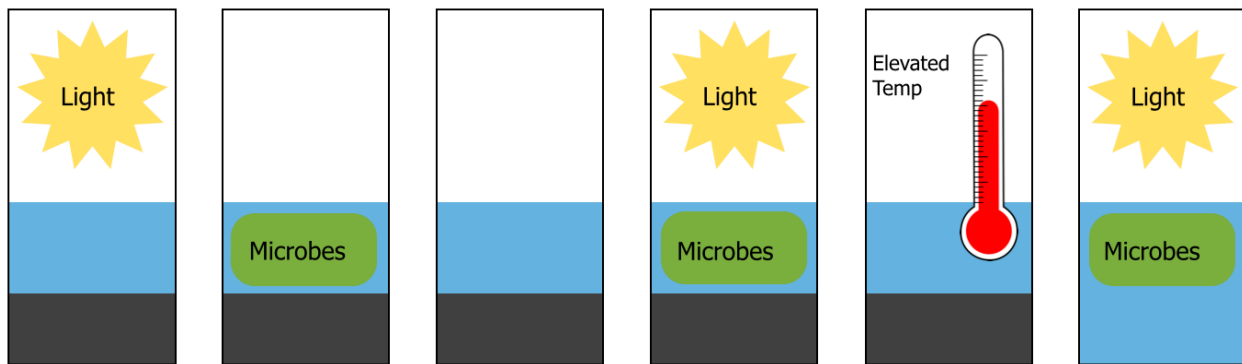


Figure 8: Sites of sample collection. PC=Pensacola, FL, FP=Fort Pickens, Pensacola, FL, PD=Perdido Key, FL, GS=Gulf Shores, AL, FM=Fort Morgan, AL, DI=Dauphin Island, AL, PG=Pascagoula, MS, BX=Porter Ave Biloxi, MS, SI= Ship Island, MS, GP=Gulf Port, MS, WL= Waveland Jetty, MS, GI=Grand Isle, LA Public Beach, Grand Isle, LA, EI=Elmer's Island, LA, PF=Port Fourchon, LA).

### **Incubation: raw oil**

Raw ocean water was collected from a pier off of Altman Playground in Atlantic City, NJ. Half of this water was sterilized using 10% sodium azide solution (3.0 mL azide solution in 30 mL water "abiotic"). Surrogate BP oil (80 mg, 100 µL) was added to pre-combusted clear or amber glass vials (see Figure 9 for sample names and assigned environmental variables). 30 mL of water was added to each sample vial (alive or sterilized based on scheme figure 9). Samples were capped with sterilized cotton plugs. One set of samples was left in a New Brunswick Scientific 12500 series incubator

shaker at 27-36°C, while the rest were left exposed to ambient sunlight. All vials were shaken once a day and water was added to maintain initial volumes. Samples were extracted at three week intervals for 15 weeks. A final set was reserved and sampled after 21 weeks.



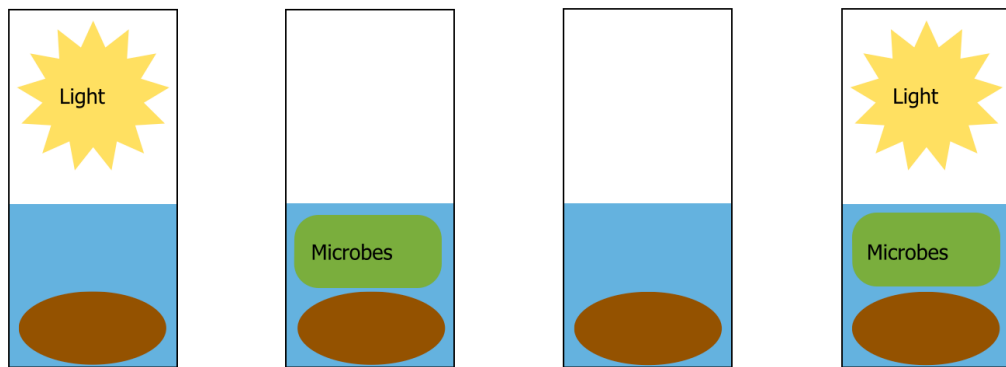
	A	B	C	D	E	F
Light	Yes			Yes		Yes
Microbes		Yes		Yes		Yes
Oil	Yes	Yes	Yes	Yes	Yes	
Heat					Yes	

Figure 9: A summary of the various raw oil incubations and simulated environmental perturbations.

### Incubation: oil soaked sand patties

The same biotic or abiotic water was used for the oil soaked sand and raw oil incubations. Samples were collected at Gulf Shores and Pensacola Beach. A few grams of each patty were placed in pre-combusted clear or amber glass vials (see Figure 10 for sample names and assigned environmental variables). 40 mL of water was added. Vials were capped with sterilized cotton plugs and left in ambient sunlight. Samples

were shaken once a day and water was added to maintain initial volumes. Samples were extracted at seven week intervals.



	A	B	C	D
Light	Yes			Yes
Microbes		Yes		Yes
OSP	Yes	Yes	Yes	Yes

Figure 10: A summary of the various raw oil incubations and simulated environmental perturbations.

### Sample extraction and preparation

Samples that needed to be stored prior to extraction were stored at -20°C. Samples were dissolved in 15 mL of 4:1 dichloromethane:methanol and centrifuged at 1600 rpm for seven minutes. This liquid extraction was done three times. The collected organic layer was extracted and passed through a column of NaSO<sub>4</sub> to remove any finer particulates and water and gathered in pre-weighted flasks. The samples were then dried under reduced pressure.

A fraction (~0.10g) of dry sample was dissolved in C<sub>2</sub>Cl<sub>4</sub> (14mg/mL). This solution was injected into the clean DCL-M25 cell. The cell was loaded into the IR chamber and purged for at least 15 minutes.

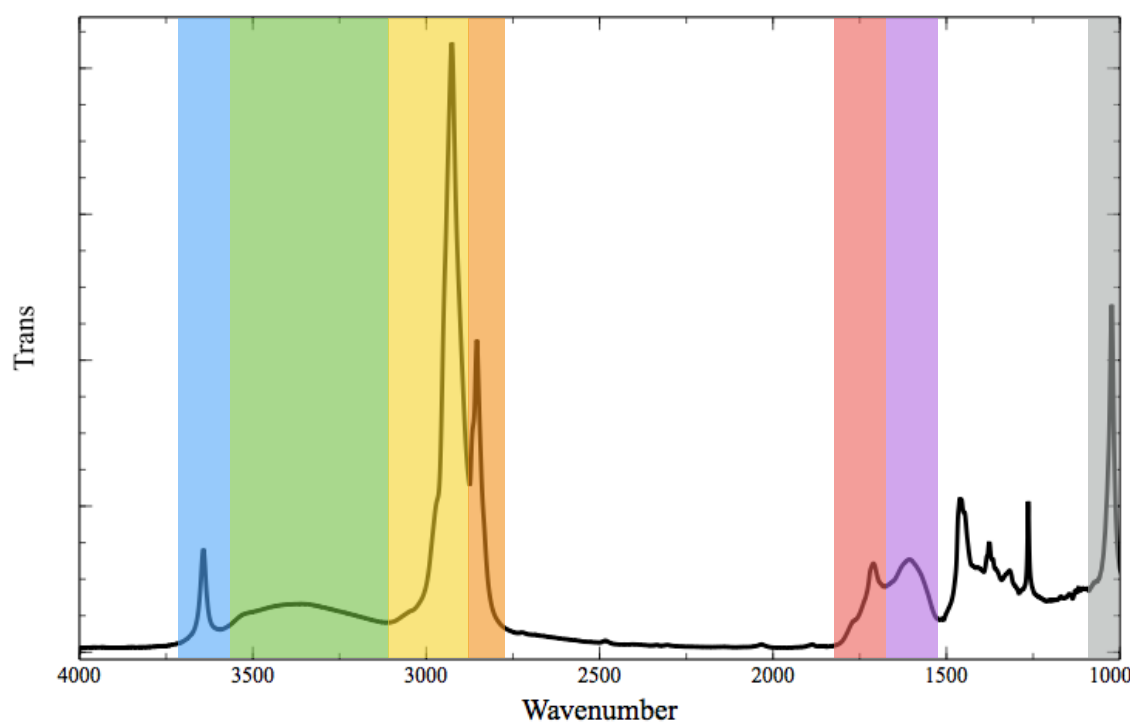
### **FT-IR analysis**

All parts of a Harrick demountable liquid cell (DCL-M25) fitted with 250 micron spacers, calcium fluoride plates, stainless steel ports, and polytetrafluoroethylene Luer fittings were rinsed three times with methanol, dichlormethane, and hexane. The DCL-M25 was assembled and then cleaned with the triple solvent system again with the addition of washing with C<sub>2</sub>Cl<sub>4</sub> as the final solvent using a 1.00cc BD Yale Tuberculin glass syringe with a glass Luer tip. All bottles of C<sub>2</sub>Cl<sub>4</sub> were kept dark.

Spectra were collected on a Thermo Scientific Nicolet 6700 FT-IR using Omnic Software, 8.0. The FT-IR used a KBr beamsplitter and a deuterated triglycine sulfate (DTGS) detector behind a KBr window. The sample chamber was purged with dry nitrogen at 40 psi using a Parker-Balston FT-IR purge gas generator. At the start of each collection day a background was collected after about 8 hours of purging. Spectra were generated using 32 scans at a 2 cm<sup>-1</sup> resolution measuring from 400 to 4000 cm<sup>-1</sup>. In reality on the region from 1000 to 4000 cm<sup>-1</sup> were processed because the CaF<sub>2</sub> plates disrupt all signals below about 950 cm<sup>-1</sup>. Between sample collections the chamber was allowed to purge for at least 15 minutes.

The max absorbance of each CH region was around 1.3. After collection, a solvent blank spectrum of C<sub>2</sub>Cl<sub>4</sub> was subtracted to remove solvent peaks, such as the triplet peak between 1100-1200 cm<sup>-1</sup>. Areas and heights of specific peaks were

integrated using Omnic software and normalized to the area of the C-H peak between 2750-3100 cm<sup>-1</sup>. Figure 11 shows wavenumber ranges for these peaks. These normalized areas and heights were then used to generate a series of internal peak ratios. These ratios were then mapped over time and across samples to find trends in oxidation. After collection, the sample was removed and the cell was again rinsed with the three-solvent system, finishing with C<sub>2</sub>Cl<sub>4</sub>.



Free OH (3658-3629 cm<sup>-1</sup>), O-H stretch (3740-3115 cm<sup>-1</sup>), asymmetric CH<sub>3</sub>/CH<sub>2</sub> stretch-referred to as C1 (3030-3877 cm<sup>-1</sup>), symmetric CH<sub>3</sub>/CH<sub>2</sub> stretch-referred to as C2 (3877-2822 cm<sup>-1</sup>), C=O stretch (1813-1670 cm<sup>-1</sup>), C=C stretch (1670-1521 cm<sup>-1</sup>), C-O stretch (1064-1006 cm<sup>-1</sup>).

Figure 11: The figure shows anFT-IR spectrum showing the areas of interest and the functional groups they represent.

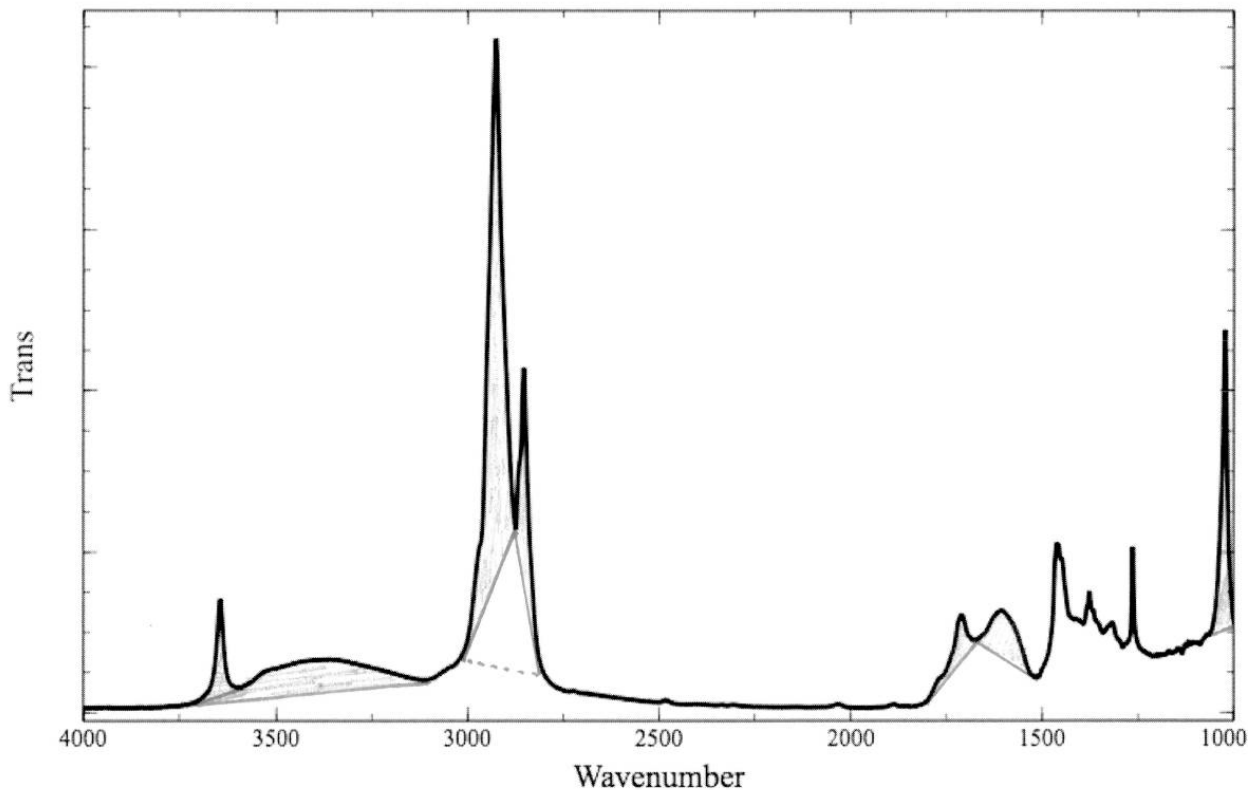


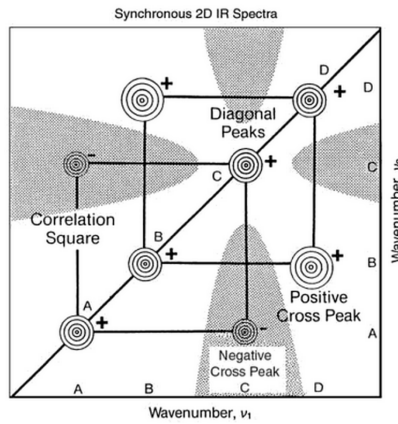
Figure 11 (cont.): The figure shows the integration scheme for all the peaks with the solid lines outlining the integration areas of selected peaks and the dotted line showing the area for the CH total integration.

### GC-FID analysis

For gas chromatography flame ionization detection 100 $\mu$ L of oil was injected and analyzed using a 1D Agilent 7890 series GC-FID. Compounds were separated on a DB-XLB capillary column (30m, 0.25mm internal diameter, 0.25 $\mu$ m film). Hydrogen carrier gas was kept at a constant flow of 1mL min<sup>-1</sup> using a Parker Balston hydrogen generator. The oven was kept at 40°C (1 min hold) and then increased at a rate of 5°C min<sup>-1</sup> to 320°C (15 min hold). Total run time was 72 minutes.

## 2D correlation analysis

Figure 12 shows the equations used to generate 2DCA plots with environmental samples.



$$\phi(v_1, v_2) = \frac{I}{n-1} y^T(v_1) \cdot y(v_2)$$

$$\psi(v_1, v_2) = \frac{I}{n-1} y^T(v_1) \cdot N \cdot y(v_2)$$

$$N_{j,k} = \begin{cases} 0 & \text{if } j=k \\ \frac{1}{\pi(k-j)} & \text{if } j \neq k \end{cases}$$

Figure 12: 2DCA equations (right) where  $\phi$  is the synchronous spectrum,  $\psi$  is the asynchronous spectrum,  $v_1$  and  $v_2$  are spectral channels,  $y$  is a vector of the signal intensities in column  $v$ ,  $n$  is the number of signals in the original dataset, and  $N$  is the Noda-Hilbert transform matrix. The graph (left) shows the synchronous spectrum and how to interpret it—where positive correlation across the diagonal represents two peaks growing or shrinking together, and negative correlation indicates one peak growing and the other shrinking at the same time.<sup>32</sup>

2DCA generates two Figures—asynchronous and synchronous spectra. The asynchronous spectra shows what peaks are related in time (one after another), and the synchronous spectra shows how the peaks are directly related (increase or decrease together). 2DCA was attempted with environmental samples and incubated samples following instructions laid out by Noda in *Two-dimensional Correlation Spectroscopy: Applications in Vibrational and Optical Spectroscopy*.<sup>32</sup> Perturbations used for environmental samples were distance from the wellhead and date collected. Time was the perturbation used for the incubated samples. The signal to noise ratio was so small and any exigent correlations so slight that this technique yielded no results.

## Results

To test the viability of FT-IR as a screening method for oil, it is necessary to delineate how the tool will be used as a successful method of analysis. Because one of the greatest issues facing environmental oil analysis is the lack of analytical procedures to detect extremely polar byproducts of weathering, FT-IR must show a sensitivity to increasing or decreasing functional groups across spectra, as well as show reproducibility with samples over time. Raw oil was analyzed both on FT-IR and the more traditional GC-FID to establish a baseline for both incubations. Both show characteristics common in fresh sweet crude oil.<sup>33</sup> Figure 13 shows the GC-FID chromatogram of raw surrogate oil. The abundance of straight-chain alkanes and small UCM indicate that the oil has undergone little to no weathering. Figure 14 shows the FT-IR spectrum of raw surrogate oil. All the peaks indicate carbon-hydrogen bond characteristics with the exception of the small peak from 1670-1521 cm<sup>-1</sup> indicating C=C bonds.

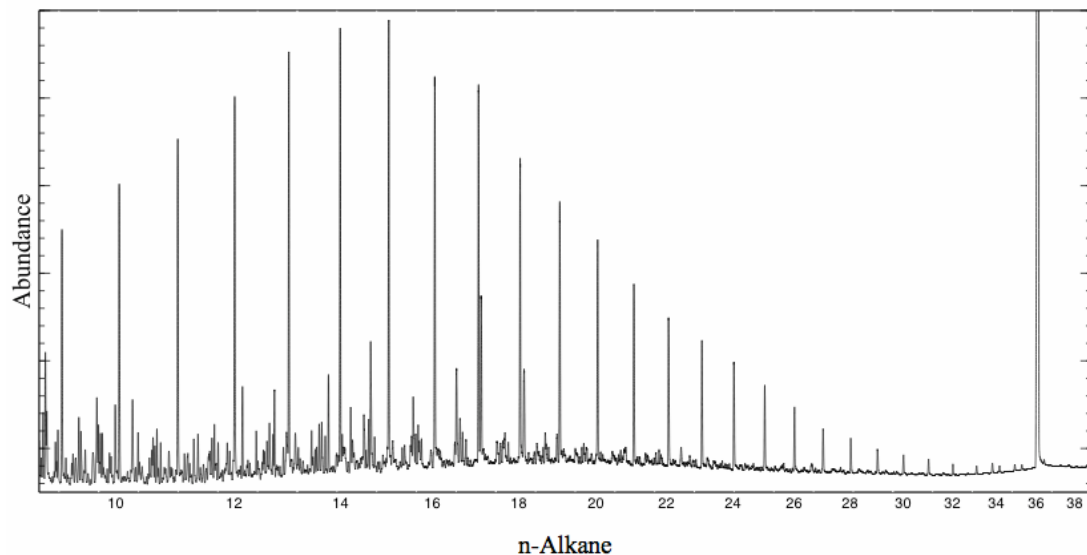


Figure 13: The GC-FID of raw surrogate oil shows characteristic abundance of both low and high molecular weight saturated alkanes, a small UCM, and confirmed pristane/phytane ratios (see appendix A).

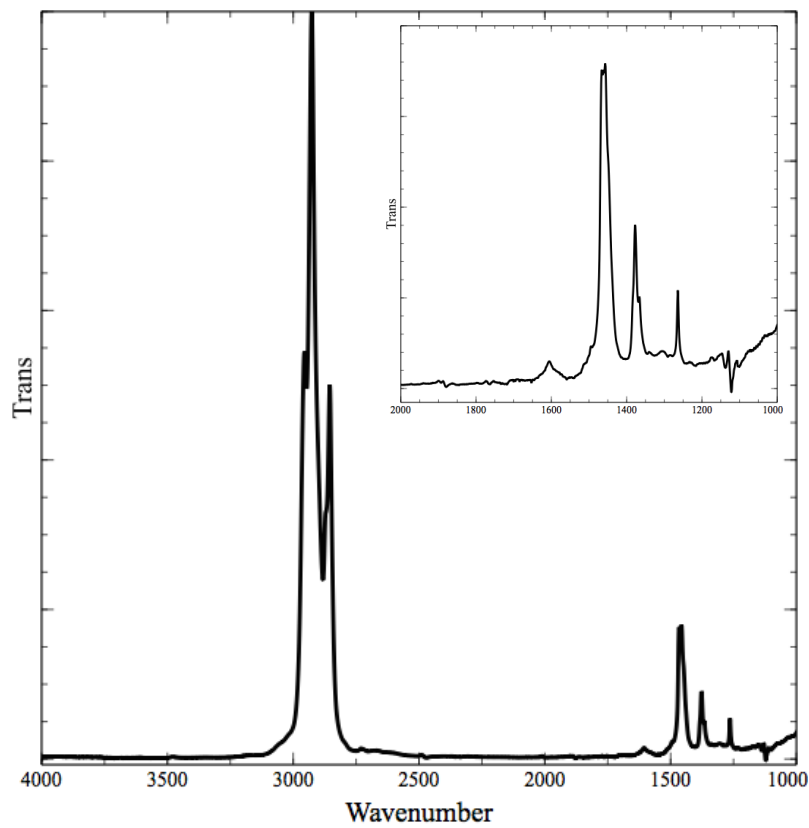


Figure 14: The FT-IR of raw surrogate oil shows an expected lack of peaks corresponding to oxidized functional groups.

## Raw oil incubation

From a purely qualitative standpoint it is clear that the incubated raw oil underwent some fundamental compositional change. Gas chromatography indicates a loss of lighter molecular weight n-alkanes ( $n=1$  to  $n=13$ ) and a more pronounced UCM—characteristic of weathered oil. Figure 15 shows the GC-FID chromatogram of a sample that has been exposed to light for 12 weeks. The depletion of n-alkanes compared to Figure 13 is clear. Pristane and Phytane were integrated on the GC-FID chromatograms, as were  $C_{17}$  and  $C_{18}$  alkanes. The Pristane/Phytane ratio was consistent across all chromatograms (see appendix A for integration data).

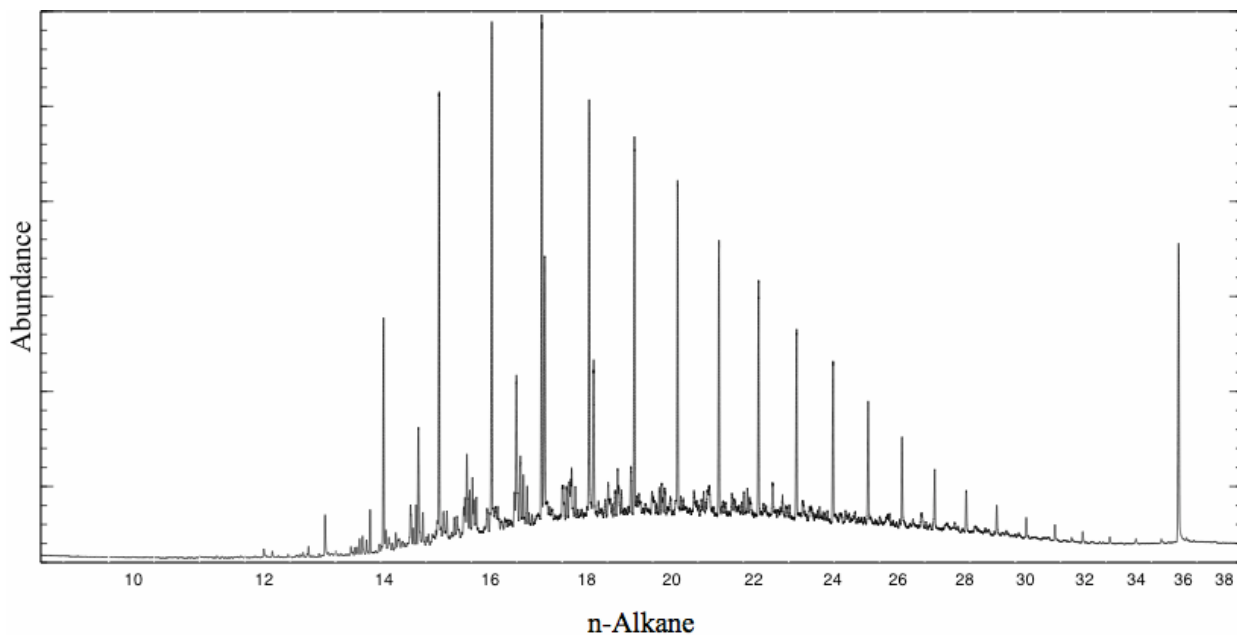


Figure 15: GC-FID chromatogram of raw oil exposed to sunlight for 12 weeks.

The IR spectra also indicates that oxidation has occurred, though this is subtle and evidenced by more pronounced C=O and C-O peaks at  $1813-1670\text{ cm}^{-1}$  and  $1064-1006\text{ cm}^{-1}$  respectfully. Both of these peaks are largely absent in the raw oil. Figure 16 show the FT-IR spectra of a sample that has been exposed to light for 21

weeks. The C=O peak is obvious, and the peak around  $1000\text{ cm}^{-1}$  may indicate the influx of C-O bonds. Data from GC-FID spectra and FT-IR confirm that the incubated oil experienced some sort of chemical process analogous to environmental weathering (at least in function if not exact intensity). The next step is to establish if these changes are gradual and measurable over time and to try and differentiate changes based on the various simulated environmental variables.

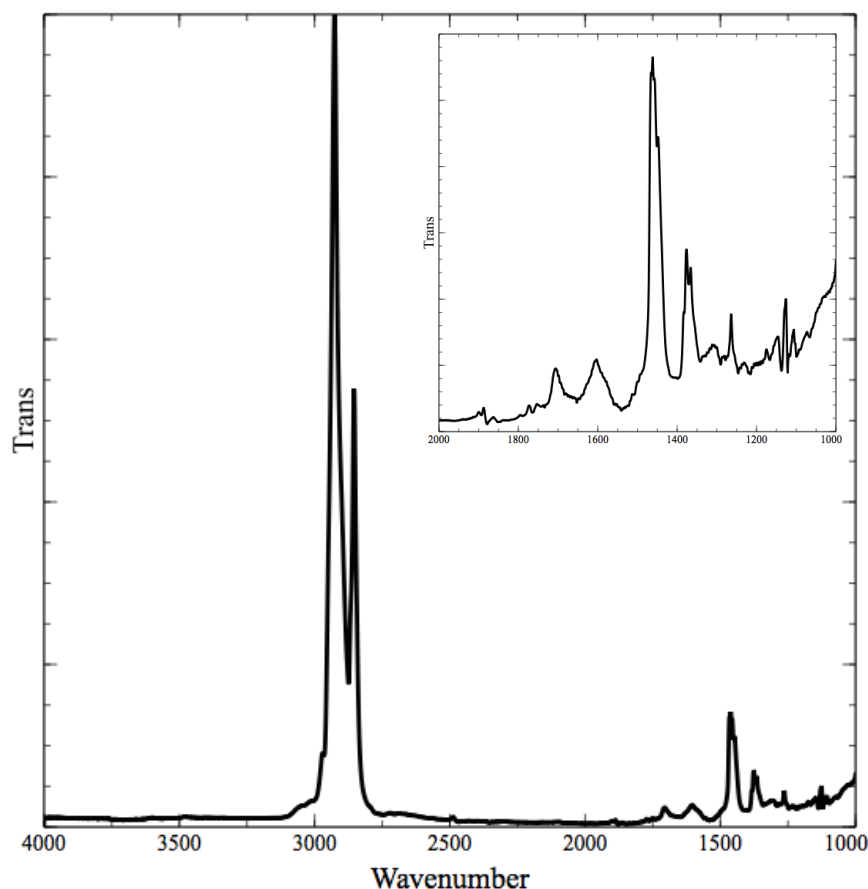


Figure 16: FT-IR spectra of raw oil exposed to light for 21 weeks.

To effectively examine temporal changes in oil incubations, internal ratios of oil including the ratio of aldehyde character to total CH<sub>3</sub>/CH<sub>2</sub> character, unsaturated hydrocarbon character to total CH<sub>3</sub>/CH<sub>2</sub> character, and C-O character to total CH<sub>3</sub>/CH<sub>2</sub>

character (see appendix D for full list of generated ratios) were used. These internal ratios represent relative compositional changes. By using internally generated ratios, inconsistencies arising from differences in spectral intensity and changes in concentration are mitigated. The most useful ratios were those that compared oxidized peaks to the total CH area (the total area under both peaks corresponding to asymmetric and symmetric methyl and methylene stretches). Other peaks, while potentially interesting from a purely chemical perspective, say little about changing levels of oxidation over time. By directly comparing the alcohol, aldehyde, and unsaturated hydrocarbon character of a sample to the saturated hydrocarbon character a clear picture of weathering can be elucidated. Other ratios are certainly worth exploring, but many showed no correlation between time and changing integrations, and are unhelpful in testing FT-IR as a method of directly tracking oxidative change in marine oil.

#### *Effects of light and dark systems*

Incubations A, C, and D were used to specifically track changes due to light (C being the dark control, A exposed to just light, and D exposed to light and microbes). GC-FID and FT-IR confirm changing levels of oxidation (specifically enrichment of unsaturated bonds and aldehydes) in A and D but not in C—indicating that oxidative changes are a product of exposure to indirect sunlight.

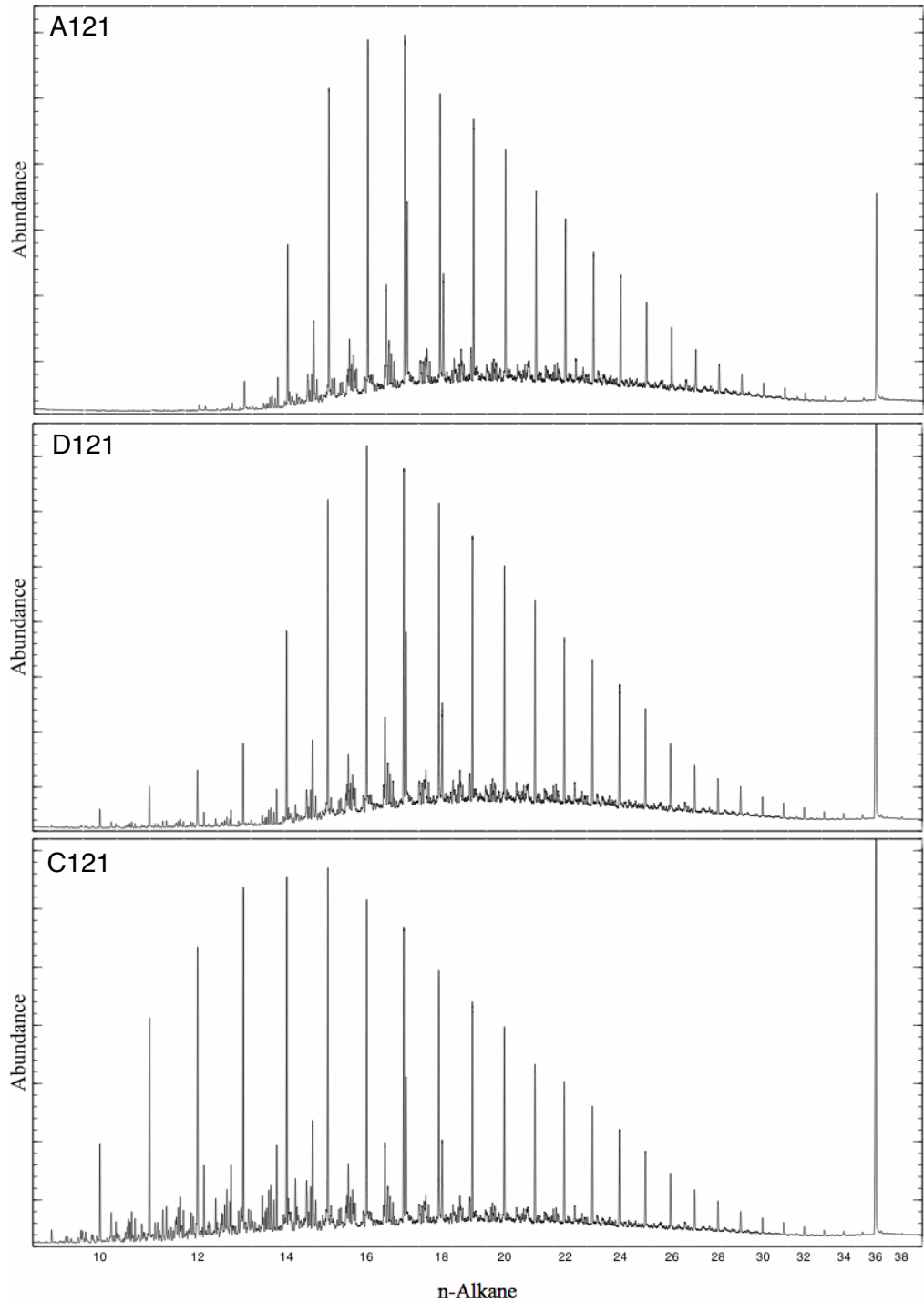
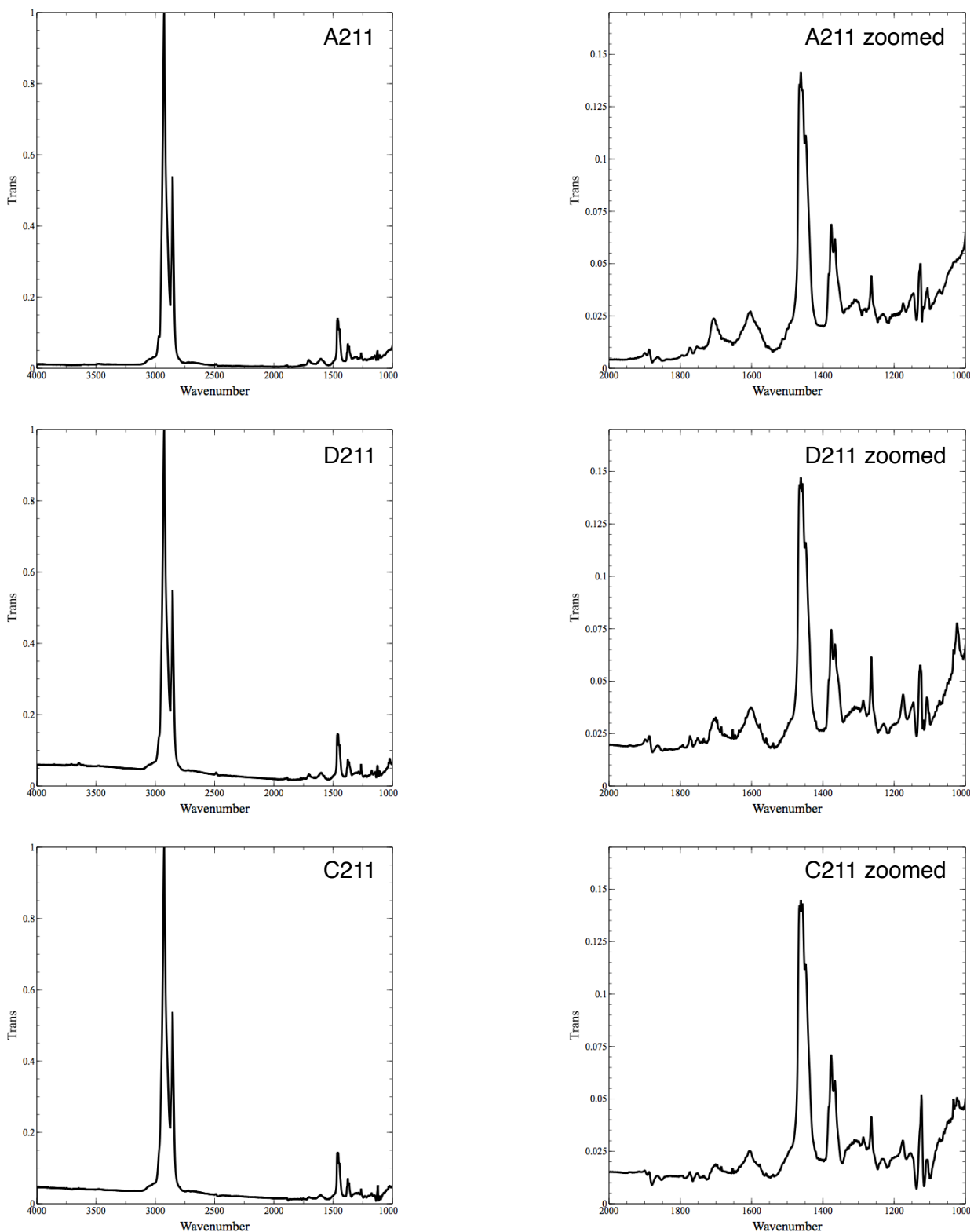


Figure 17: GC-FID (12 weeks exposure) and FT-IR (21 weeks exposure) of raw oil incubations A (light, abiotic), D (light, biotic), and C (dark, abiotic).



**Figure 17 (cont.):** FT-IR spectra showing a full spectral view (left) and a zoomed in window to highlight the C=O, C=C, and C-O peaks.

Figure 17 shows the FIDs and FT-IRs of incubated samples. Visually, it appears that there is a loss of lighter molecular weight hydrocarbons. This was not unexpected—one of the most recognizable indicators of oil weathering is the loss or complete absence of n-alkanes. More interesting is the retaining of n-alkanes n=13 through n=16 in the light and biotic sample (D) and the absence of these saturated hydrocarbons in the sample only exposed to light. The FT-IR also visually show subtle differences in C=O, C=C, and C-O peaks.

While the GC-FID spectra offer an interesting insight into the non-polar changes in incubated oil, after a certain amount of time no change is seen as the polar components are not GC-amenable. FT-IR shows the changes in the polar fractions of oil. Using peak heights is one method of measuring functional group abundance. Figure 18 shows four peak heights and how they change over time when the sample is exposed to light. Heights are based on distance from the peak in question to the C1 peak using the spectra normalized to the CH peak height. The difference between C1 (defined as 2924 cm<sup>-1</sup>) the C=O height (peak at 1704 cm<sup>-1</sup>), the C=C height (peak at 1604 cm<sup>-1</sup>), the C-O height (peak at 1028 cm<sup>-1</sup>), and the C2 height (peak at 2853 cm<sup>-1</sup>) was taken from the .csv files of the spectra and visualized.

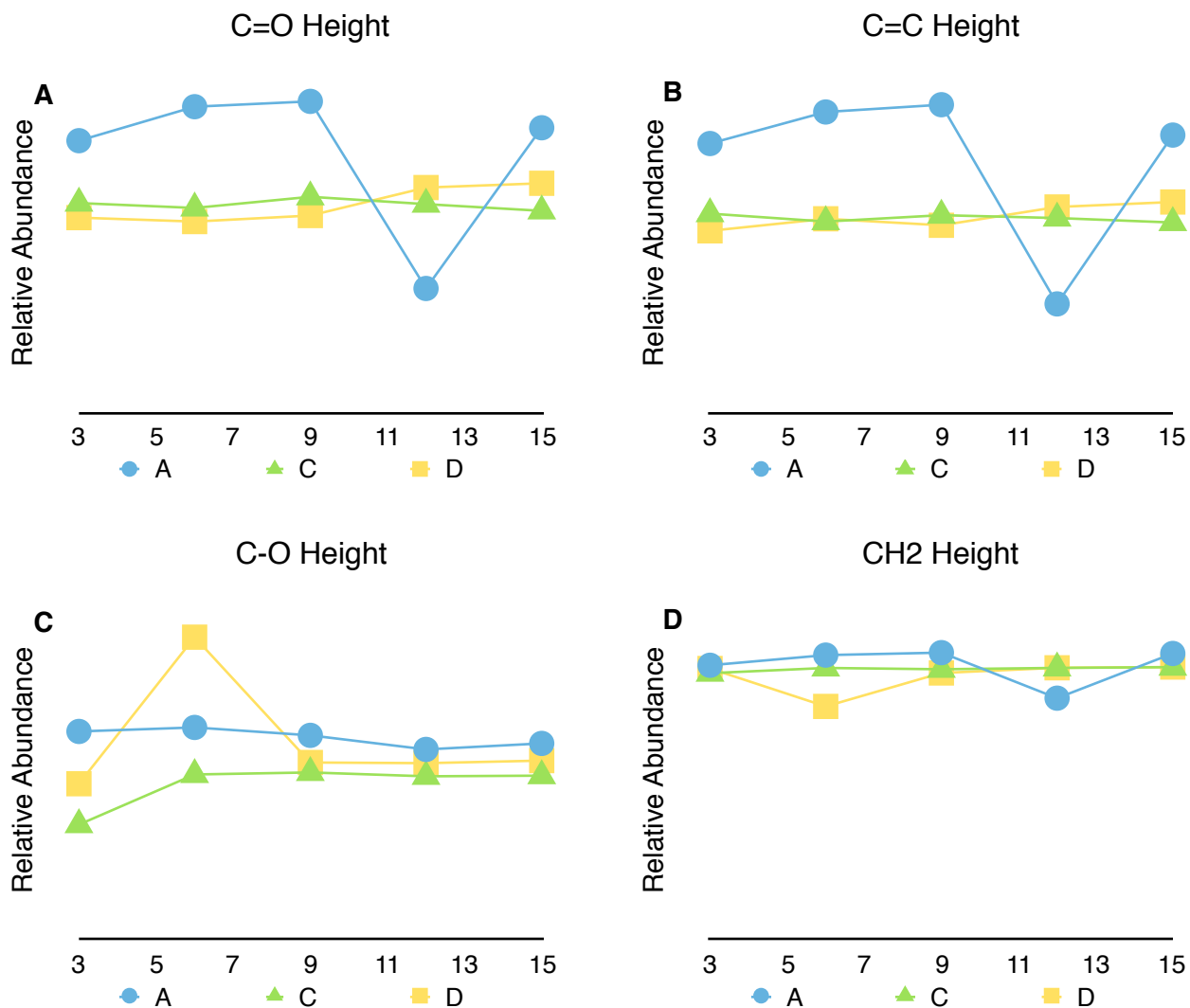
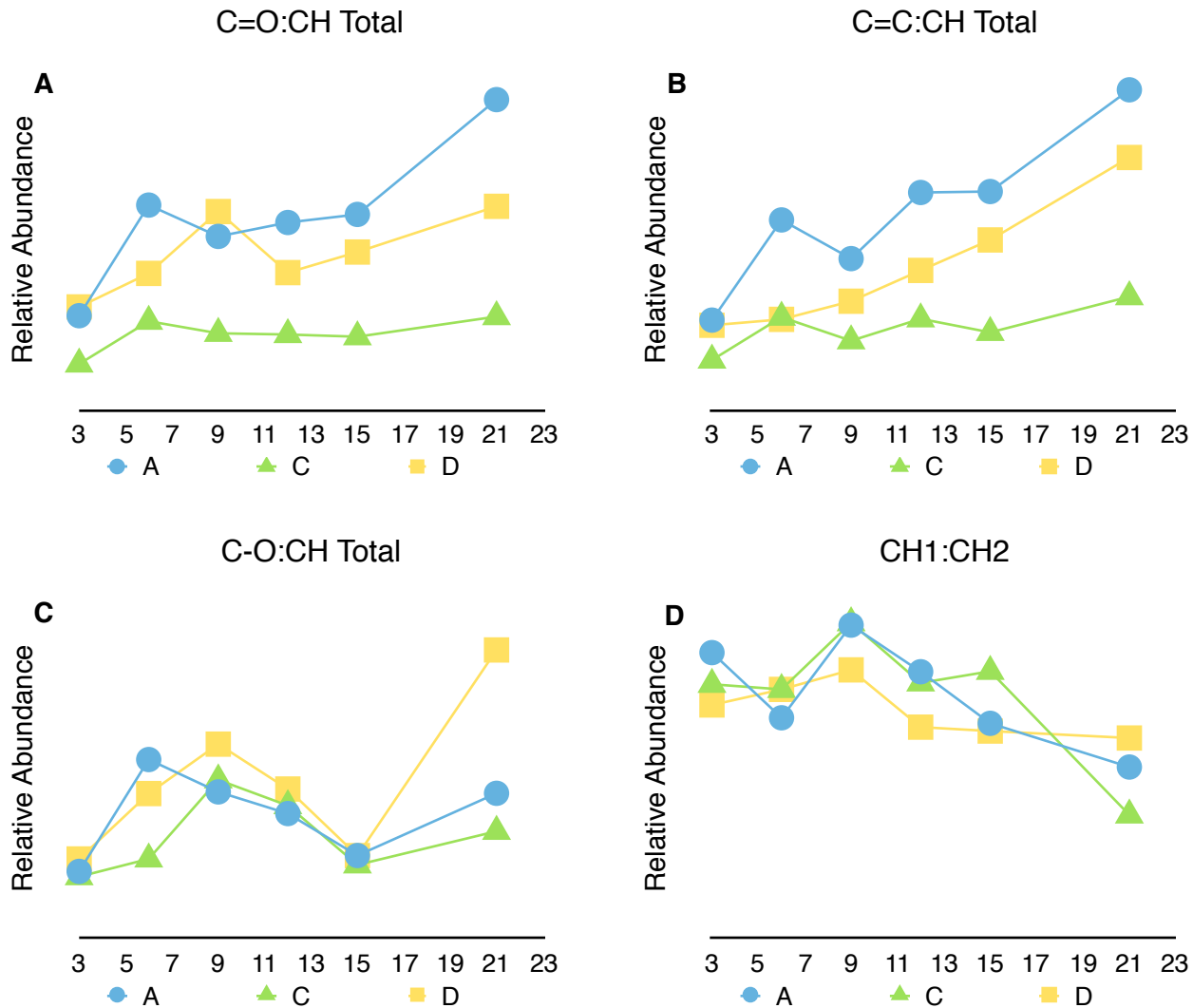


Figure 18: FT-IR peak heights. X-axis represents weeks incubated.

The peak heights are largely stable over time. This would indicate that oil barely changes, or that all the changes happen within the first three weeks of exposure. The limitation of peak height is that it only tests one specific chemical environment. The same functional groups on different compounds can have slightly different chemical shifts. Thus isolating one high point is not a good method for testing total abundance of a specific functional group in a heterogeneous mixture like oil. Peak areas, shown in Figure 19, were also measured to see if they would provide further information regarding chemical change over time.

Figure 19: Internal ratios of FT-IR integrations exposed to light. X-axis represents weeks incubated.



The C=O:CH total ratio is perhaps the best indicator of oxidative weathering. The dark control (Figure 19, green lines) remains fairly steady over the 21 weeks. Both A and D follow upward trends ( $r^2$  values of 0.75 and 0.51 respectively), indicating that over time the samples are enriched with aldehyde-based functional groups (Figure 19a–blue and yellow lines). The ratio of alkenes to total carbon content also follows a strong upward trend in both A and D ( $r^2$  values of 0.87 and 0.95 respectively) while the control

remains steady as seen in Figure 19b. Exposure to light can result in decreasing levels of unsaturation in oil. This is important because alkenes are more reactive than alkanes and thus more likely undergo further reactions over time than their saturated counterparts, leading to more weathering byproducts.

Over time it appears that the levels of C-O bonds in all samples remain reasonably consistent. A and D mirror the changes in the control ratios across the entire 21 weeks (Figure 19c). The two carbon peaks appear to maintain a similar relationship as well over time (Figure 19d). This is to be expected, and there is no reason to assume the ratio of symmetric to asymmetric stretching in bulk oil would change over time, but it is also a useful control to make sure trends are not being imagined across other ratios.

Light seems to generate an increase in the abundance of C=O and C=C functionality while having minimal effect on the C-O or the various carbon-hydrogen abundances.

#### *Effects of biotic and abiotic systems*

Samples B, C and D were used to track changes due to biology in raw oil samples. Overall chemical changes appear to be at most more nuanced and potentially absent when compared to the effects of light on raw oil.

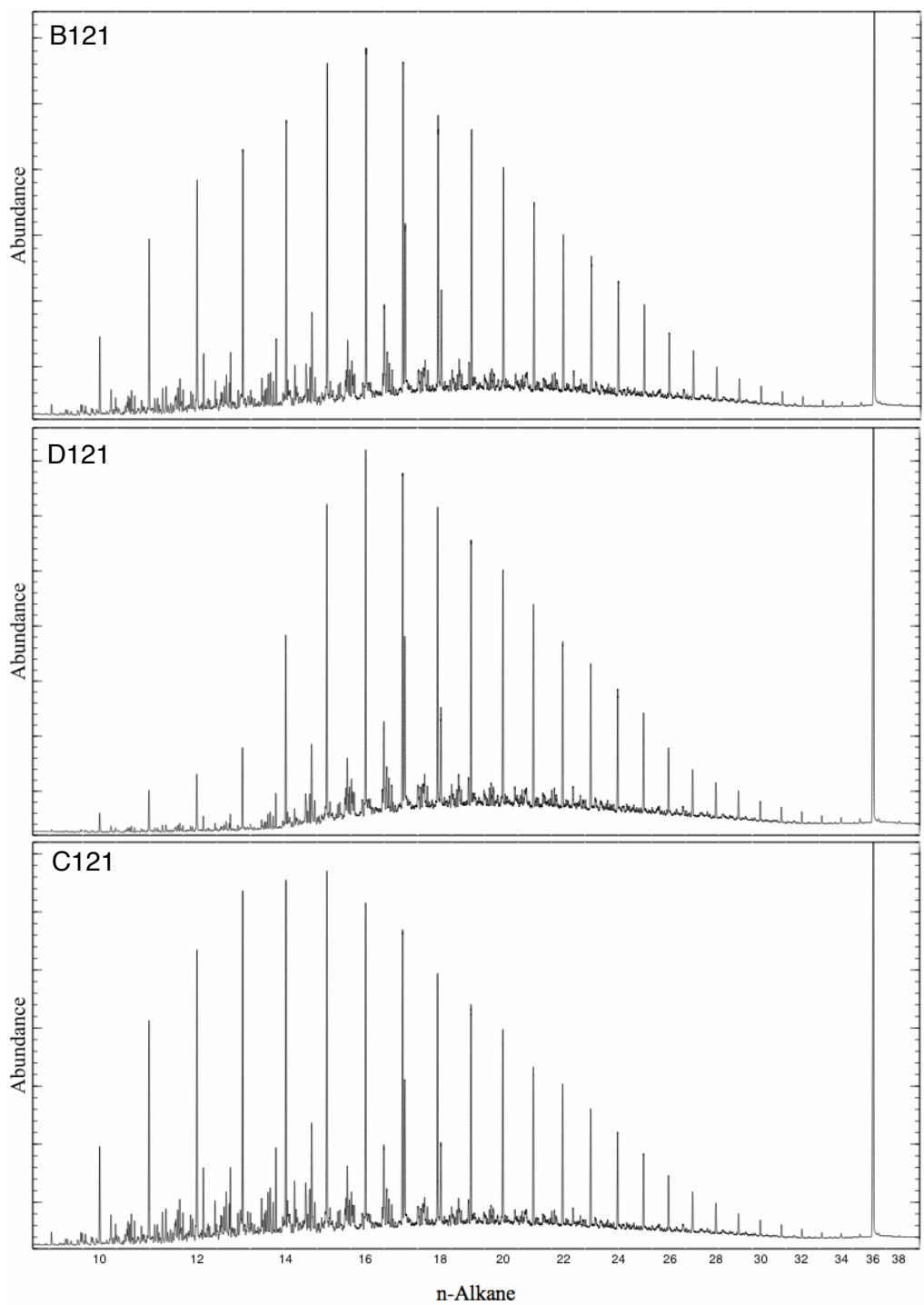


Figure 20: GC-FID (12 weeks exposure) and FT-IR (21 weeks exposure) of raw oil incubations B (dark, biotic), D (light, biotic), and C (dark, abiotic).

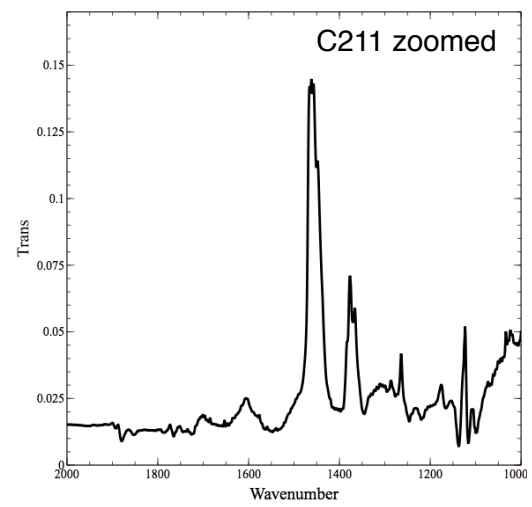
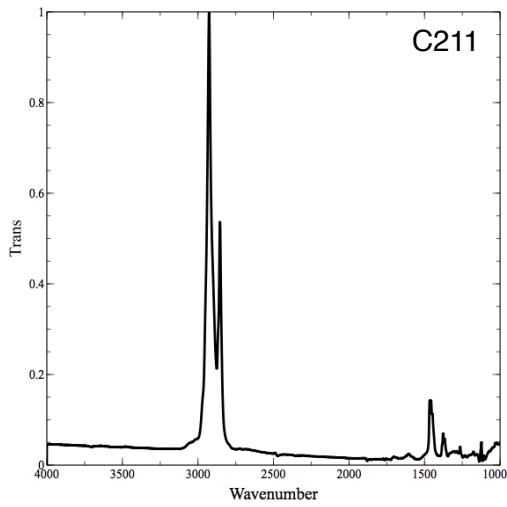
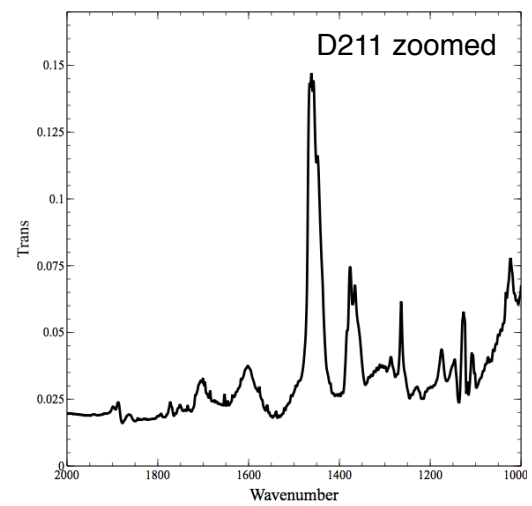
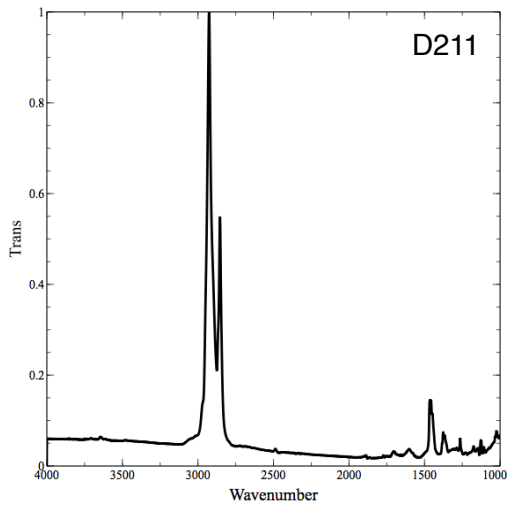
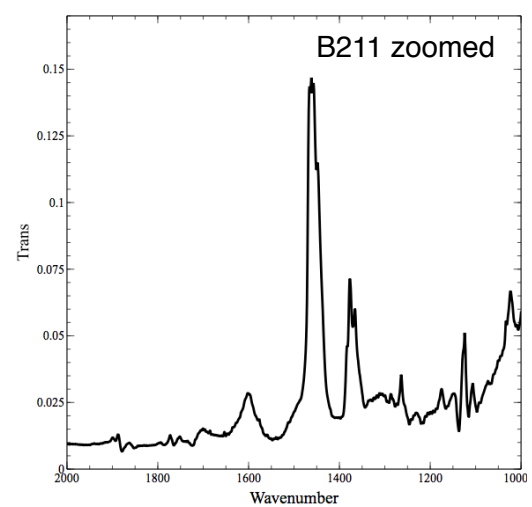
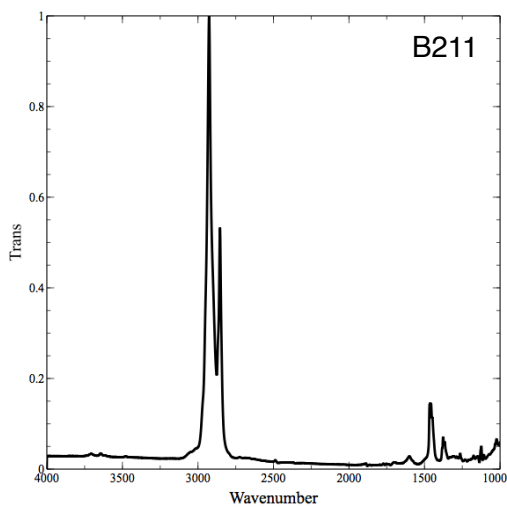


Figure 20 (cont): FT-IR spectra showing a full spectral view (left) and a zoomed in window to highlight the C=O, C=C, and C-O peaks.

The GC-FID of samples containing microbes show some loss of light-molecular weight alkanes, but much less pronounced than the samples exposed to light (Figure 20 compares a sample containing microbes, a sample exposed to light and microbes, and a dark control). The UCM is also less prominent (Figure 20 B121). The FT-IR also visually show subtle differences in C=O, C=C, and C-O peaks. While there are very few changes it is important to realize that the microbes in these samples were not fed anything but oil over the course of five months. Oil as an exclusive food source is not something most bacteria experience and thus it is not unexpected that metabolic processes appear to show less activity than reactions catalyzed by light.

Like Figure 18, Figure 21 shows the peak height of various oxidative peaks as a function of time. Heights are based on distance from the peak in question to the C1 peak using the normalized spectra. Again these lines are almost completely flat, once again proving that peak height is an unreliable technique to measure oxidative weathering. Instead, Figure 22 shows integrations of peak areas to better elucidate changes over time in raw oil exposed to microbes.

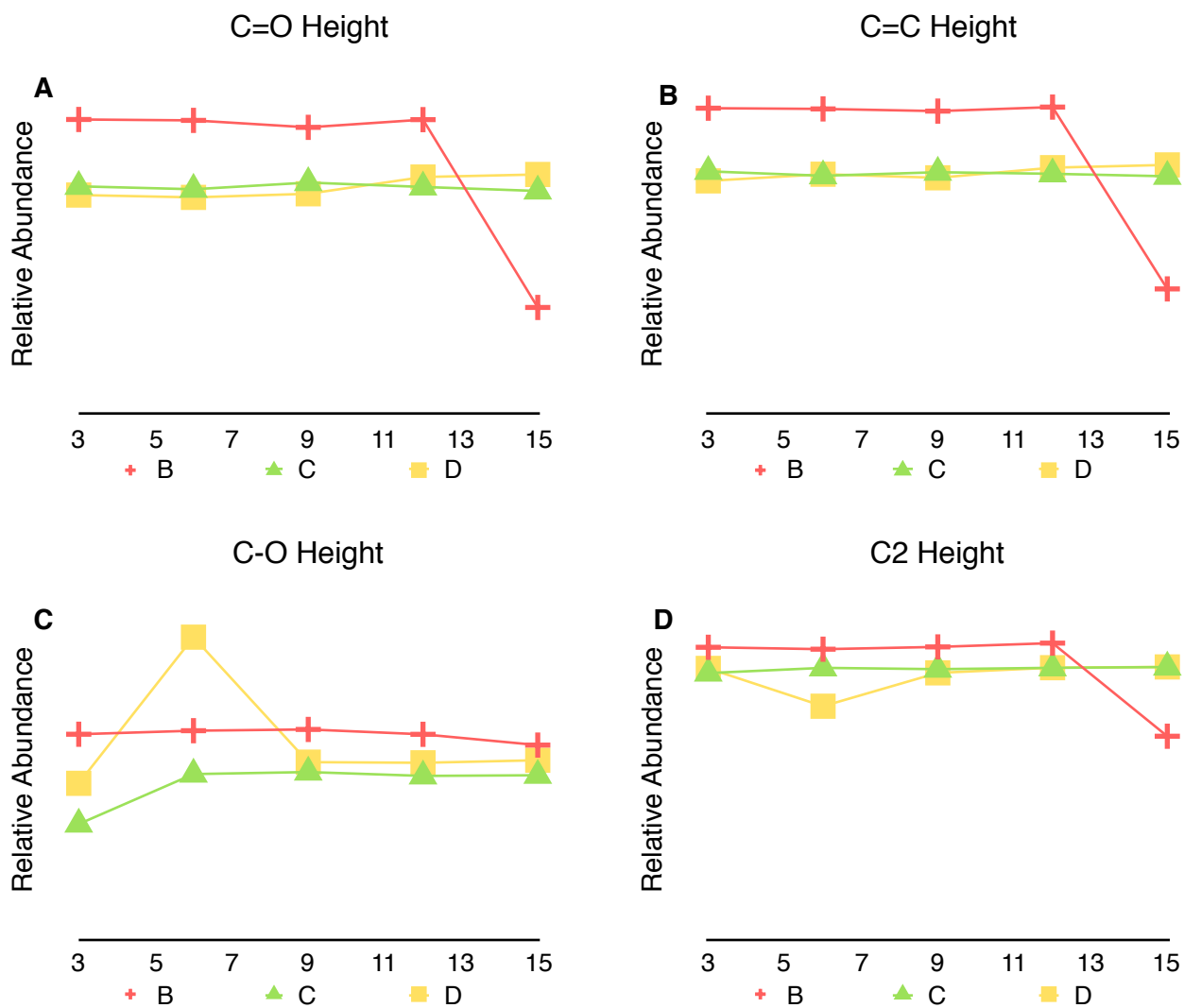
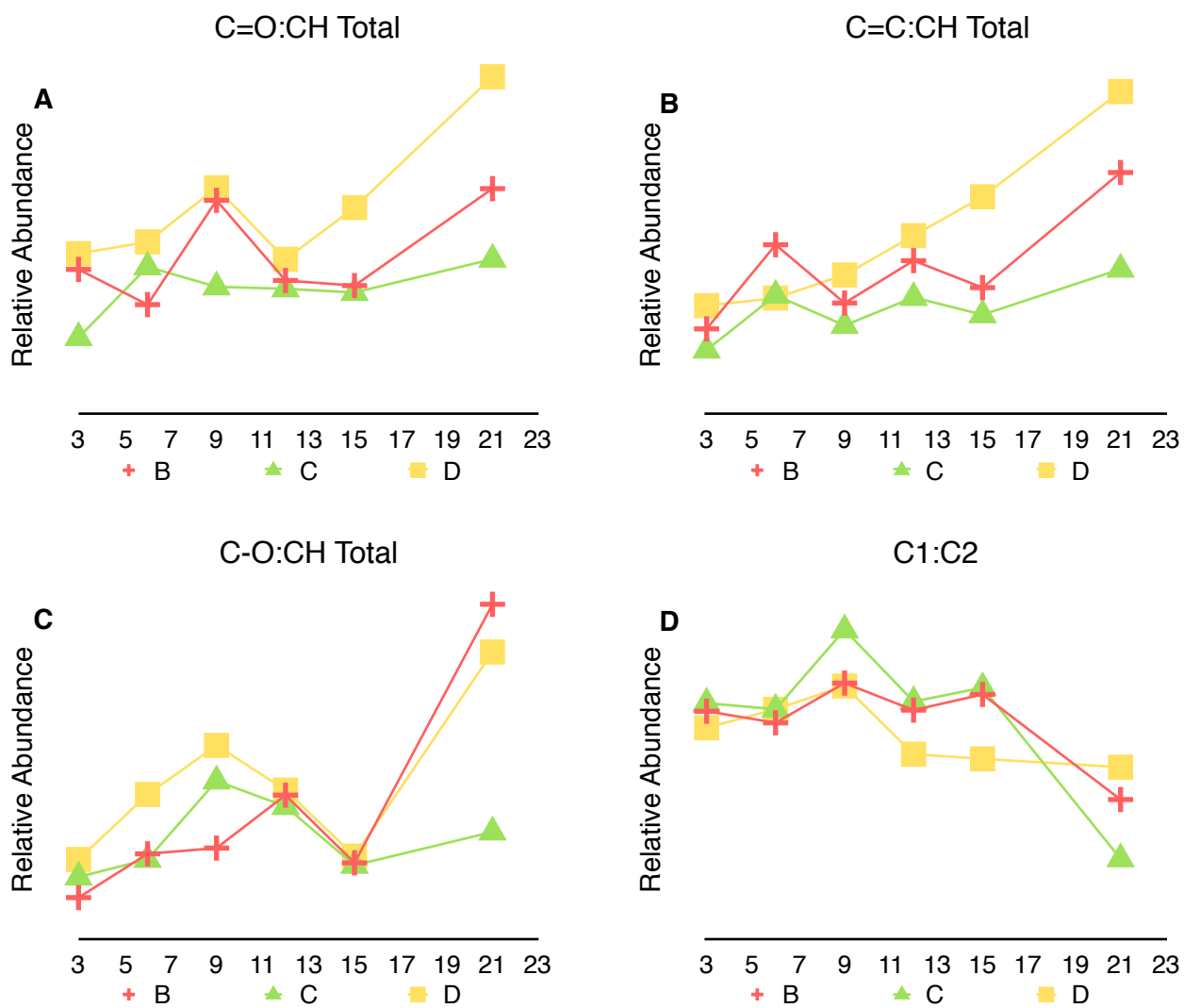


Figure 21: FT-IR peak heights. X-axis represents weeks incubated. Once again the peak heights over time of samples exposed to microbes are very stable. Peak integrations need to be used to test a broader range of functional group environments.

In Figure 22a, sample B follows a linear upward line with an  $r^2$  value of 0.25, showing little to no correlation between C=O abundance and time when compared to samples exposed to light. There is an increase in the C=C ratios (Figure 22b) of sample B, fitting a linear trend with an  $r^2$  value of 0.56 suggesting a possible, but slight, correlation. The O-C and C1:C2 ratios also show no clear correlation (Figure 22 c and d). It would appear that biology has less of an effect on oxidative levels over time—or the



changes are too nuanced to detect via FT-IR.

Figure 22: Internal ratios of FT-IR integrations. X-axis represents weeks incubated.

#### *Raw oil incubation summary*

When looking at the GC-FID and FT-IR spectra there are obvious visual differences that happen over time. However, they are small and the signal-to noise ratio for the FT-IR data makes it difficult to observe significant changes or quantify them reliably. That being said, changes in C=O and C=C integrations were measured and a correlation could exist. It also appears that samples exposed to light undergo more weathering than those exposed to just biology. Light may play a more important role in the degradation of oil. Relying on peak heights is not a viable method of quantifying levels of oxidation and instead using peak areas is a better technique. Future work should focus on expanding the time frame of incubations or using more stringent environmental variables to try and overcome these subtleties and see if clear levels of oxidation can be measured.

#### **Oil soaked sand incubation**

The above data regarding raw oil incubations show that oil can be weathered, albeit subtly, in a laboratory setting. The characteristic IR peaks do develop slowly over time. As already noted, peak oxidation level in environmental OSPs are around 70%. It would be worthwhile to test if this is simply an artificial function of sample size and location, or to see if this is actually the physical limit of oil oxidation. Thus a second incubation is necessary—this time to see if it is possible to weather OSPs.

For this incubation two OSPs from geographically distinct locations were used. One from Elmer's Island, Louisiana and one from Pensacola Beach, FL. The original

OSPs were examples of patties at the high end of the weathered spectrum. The sample from Pensacola beach had polar fractions that combined made up 72% of total oil mass, while the Elmer's Island sample had a combined polar fraction of 68% total oil by mass. Thus any oxidative weathering in these samples could be seen as an augmentation of environmental processes, rather than a continuation.

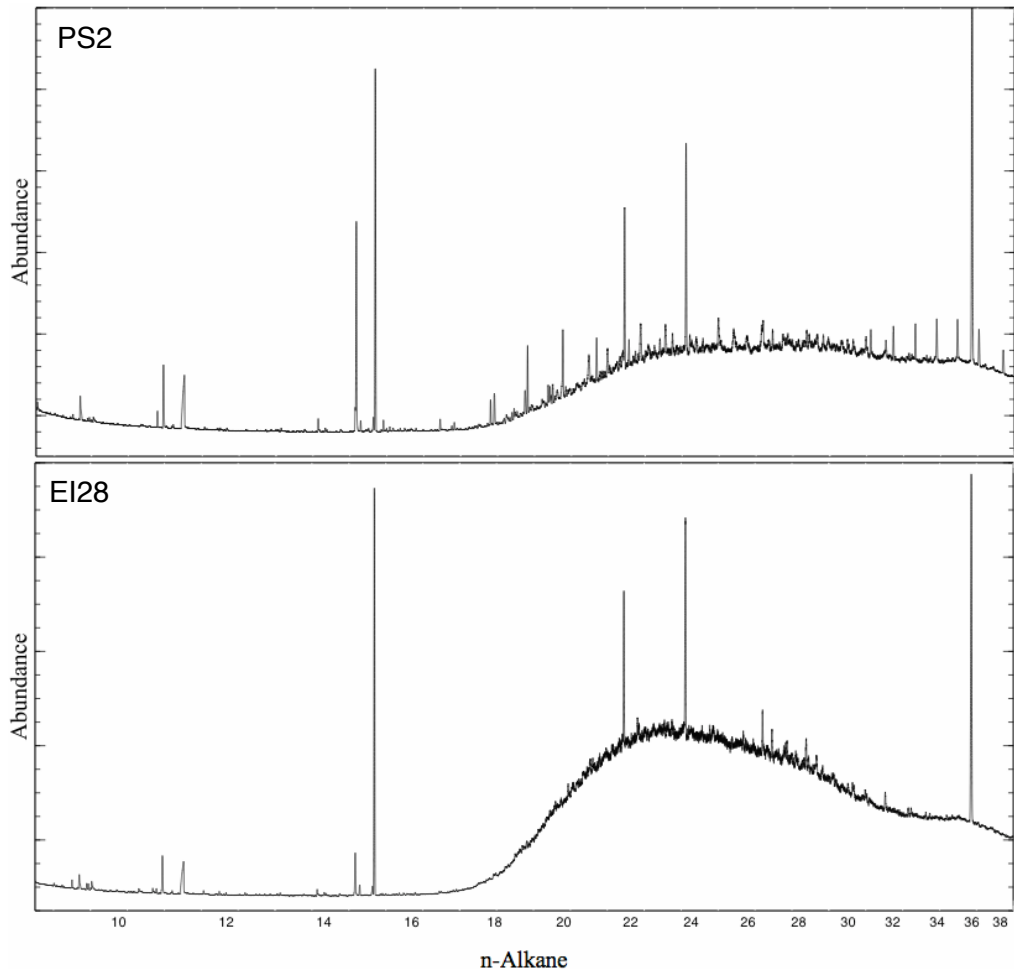


Figure 23: GC-FID plots of the two OSPs used in the incubation.

Figure 23 shows the chromatograms of the two OSPs used in the incubation. The GC-FID chromatograms are perfect examples of why new methods of oxidative detection are necessary when analyzing environmental oil. There are almost no n-

alkanes and the UCM comprises the bulk of the chromatogram. Figure 23 is useful in confirming that the sample is indeed weathered oil and could be used for biomarker analysis, but unhelpful if polar byproducts of petroleum degradation are the analytical targets. Thus FT-IR can be a useful tool in exploring degrees of oxidation within these two samples.

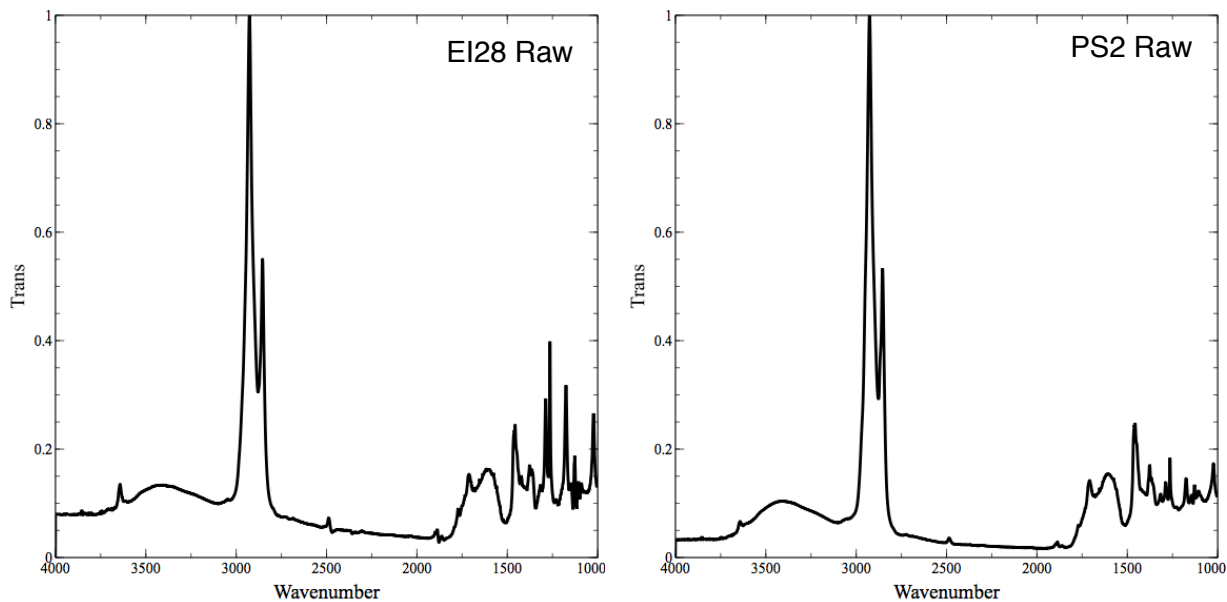


Figure 24: Initial FT-IR spectra of the two OSPs used in the incubation.

The FT-IR spectra in Figure 24 are standard examples of end-member weathering in OSPs. There are clear free OH, O-H, C=O, C=C, and C-O peaks in both samples. The incubation will test to see if these samples have indeed plateaued in their weathering, (as it appears they have from other environmental data suggesting that a 70% polar fraction is the upper limit), or if they can be oxidized further in a laboratory setting.

### *Effects of light and dark systems*

Figure 25 shows the same IR integrations used in the raw oil incubations.

Sample A was exposed to light, sample D was exposed to light and microbes, and sample C was the dark control. Data from both OSP SP2 and OSP EI28 are shown.

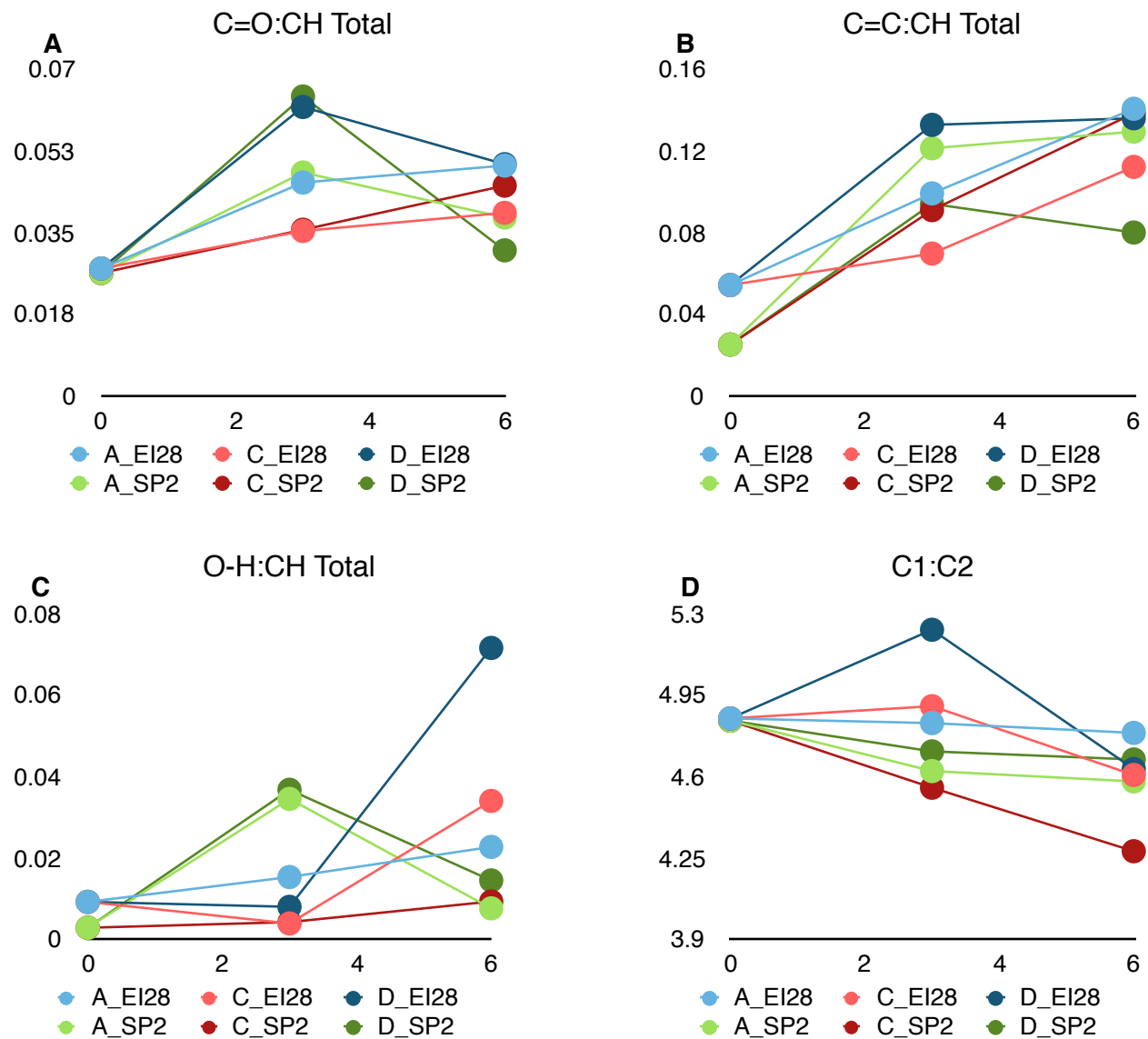


Figure 25: Internal ratios of FT-IR integrations. (T3=21 weeks of exposure and T6=42 weeks exposure).

While Figure 25 shows possible positive correlation between C=O and C=C integrations and time (Figure 25 a and b), the negative control (sample C) which was kept both dark and abiotic falls within these upward trends as well. This could mean that either nothing happened, as all data falls within the range of the control, or simply exposing OSPs to water for 10 months is enough to cause these changes. It could be that the weathering limit of the OSPs has been reached and oxidation just did not occur in measurable amounts. Alternatively, it could be that some products became so weathered that the compounds became soluble in water and thus stayed in the aqueous fraction of the liquid-liquid fraction and we not analyzed. An extraction and analysis of the water used in the incubations would be helpful in identifying the existence of these compounds.

*Effects of biotic and abiotic systems*

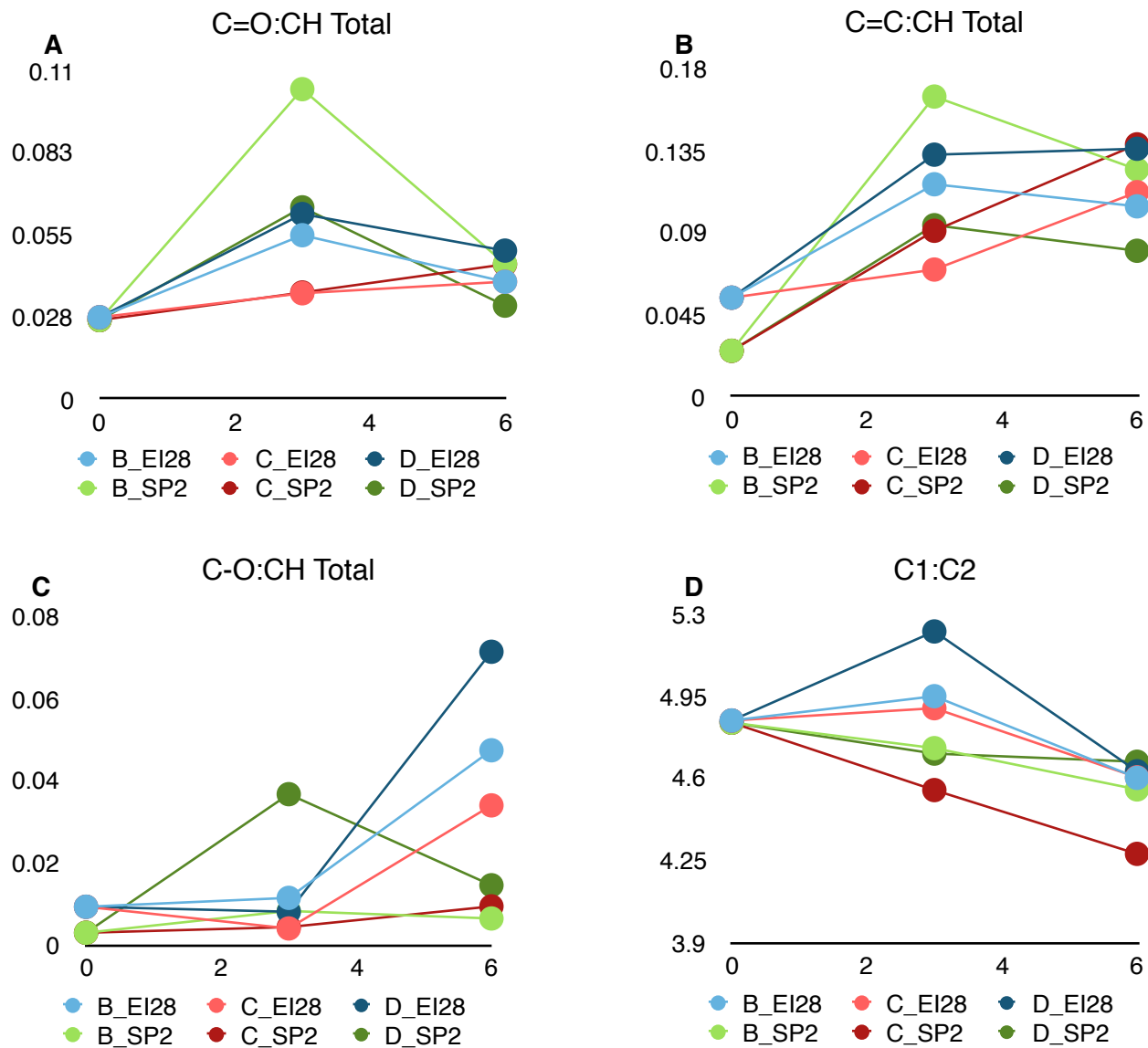


Figure 26: Internal ratios of FT-IR integrations. (T3=21 weeks of exposure and T6=42 weeks exposure).

Similar to samples exposed to light, those OSPs exposed to microbes show some positive correlation to the C=C integrations, though not as strong a correlation to the C=O integrations (Figure 26 a and b). This pattern is also seen in the raw oil incubations as well. However, like those samples exposed to light, the control samples fall in with the other data, meaning it is nearly impossible to discern changes due

specifically to the simulated environmental factors or changes due to prolonged water exposure.

#### *Oil soaked sand incubation summary*

The OSP incubation, while not wholly inconclusive, does not provide the same definitive data of the raw oil incubation. It appears that there are some increases in weathering over time correlating to C=O and C=C integrations, but because the control samples (dark abiotic) are within the range of other data, there is no clear way of determining what causes these changes, or if they are simply noise within an unchanging data set.

Once again with this OSP incubation, the limits of GC-FID have been documented in regards to analyzing heavily weathered oil. This is a reason why FT-IR could be a useful tool in characterizing bulk weathering of both lab-based incubations, and environmental samples.

## Discussion

The incubation of raw surrogate oil suggests that weathering patterns can be mimicked in a laboratory setting. Specifically there was a positive correlation over time with the abundance of C=O and C=C functionality for samples exposed to light, while only the C=C integration was strong for samples exposed to microbes. It was also shown that peak height is not a good indicator of functional group abundance as it only accounts for a small fraction of specific chemical environments. While increases in FT-IR peak areas were subtle, differences can be monitored. However, real-time “natural” environmental weathering proxies take much longer and the degree of changes seen do not coincide with the changes seen in environmental samples. Other studies have been successful in mimicking natural degradation as stated earlier.<sup>3124</sup> In a natural setting, Aeppli et al. saw more substantial changes in GC-FID, TLC-FID, and FT-IR between raw oil and surface slicks, a time difference of a few hours at most between wellhead and surface.<sup>25</sup> Studies have found detectable changes in oil at a fraction of the time scale of this study. However, other studies were using direct unfiltered sunlight, high concentrations, and high pressures. It should also be noted that none of the studies to date have attempted to establish a weathering gradient of DWH oil.

The incubation of OSPs was productive in the sense that it most likely confirmed the weathering plateau noted in Aeppli et al. study of various samples collected 18 months after the DWH spill. Their study found that most oxidative weathering products formed within 100 days of the DWH spill (amounting to  $57 \pm 4\%$  by mass via TLC-FID). OSPs collected between June 2010 and July 2011 saw only small increases in polar fractions ( $59 \pm 5\%$  by mass), with the upper limit of oxidative weather being OSPs

collected in November 2011.<sup>25</sup> These large changes seen early on after oil was released most likely has to do with the environment the oil experienced. The oil started at a depth of about 1500 m, which means the oil was under a lot of pressure before rising to the surface. Once oil surfaced, it was exposed to direct sunlight, turbulence from wind and waves, and it had a large surface area which meant more interface interactions between water, light, and oil. While the incubation discussed in this study exposed oil to sunlight and water, it was indirect sunlight through a window so most UV light was filtered out and the oil was only shaken once a day. The oil was simply exposed to less stringent weathering mechanisms. This could explain the slight (possibly negligible) increases in oxidative weathering seen in this study. Small positive correlations were shown between time and C=O and C=C integrations, but not above the range of negative controls. It would appear that OSPs cannot be weathered further, or at least to a degree that FT-IR can detect.

It should be noted for both incubations that this study was by no means an exhaustive statistical exploration of all data. The focus was to test if FT-IR could work as a generic screening method for environmental samples to measure bulk oxidative weathering. Though 2D Correlation Analysis ultimately failed in elucidating spectral relationships in a more automated way than picking peaks by hand, other numerical analysis methods could still be fruitful.

This study one again confirmed that GC-FID is an ill-equipped technique to directly measure polar functionalization of oil. Where the industry standard for oil analysis has been GC-FID, this study suggests that FT-IR could be the method of characterization for more weathered oil samples. While FT-IR will not be able to explore

the chemical composition of oil at a depth beyond general functional groups, it is a good tool to document overall oxidation and identify samples to establish what ones are worth a more in-depth analysis with more specific instrumentation.

## Future directions

FT-IR is a good tool for screening individual samples, but is limited by its general sensing of functional groups, not individual compounds. A more robust method of analysis is necessary, especially if IR spectra are to be used as the main source of weathering data. 2D correlation analysis (2DCA) was not effective with the signal-to-noise ratio of this experiment, but with larger oxidative changes, it could be a useful method of extracting time dependent changes from IR spectra. The idea is that the various IR spectra can be combined into a single matrix and then a perturbation vector can be applied that measures degrees of variation from some spectral average. This way correlations between spectral changes and the chosen perturbation (time, temperature, pH, geography) can be made obvious. Structurally this is similar to three dimensional NMR spectral analysis (COSY, NOSY) and there is precedent for using 2DCA to analyze functional group changes and chemical relationships over time via IR.

Because change in levels of oxidation were so slight in these incubations, it was impossible to establish a time-dependent gradient that could be useful in analysis of environmental samples. To generate a useful system of weathering indices, a more stringent method of weathering would be required—a longer time frame would also be beneficial to extending data. Further studies could involve irradiation of samples instead of simple exposure to sunlight, feeding and oxygenation of microbes to promote bioactivity, keeping samples at pressure, constantly moving, or managing salt concentrations and pH of the water fraction to speed up and better emulate natural factors. This could be useful in creating a better spectrum of oxidation without having to do the experiment in “real time.”

Establishing a gradient based on measured quantities of oxidized petroleum products could also be useful. Creating cocktails of standards (various carboxylic acids, unsaturated hydrocarbons, alcohols) at different concentrations and measuring changing IR integrations and then constructing a library of these peaks and their characteristics could help in identifying contributing compounds in environmental samples.

This incubation and method of extraction also ignores the water fractions. This is an obvious oversight when the experiment is exploring hypothesized increases in polarity due to weathering. As compounds degrade and become more polar, they could become water soluble and thus this method falls short. A simple next step would be to extract the water fractions and look at the samples via GC-FID, GC-MS, and FT-IR.

Though FT-IR can be used as screening tool, more precise analytical techniques are still necessary to explore the polar fractions of oil.

## Works cited

1. Camilli, R.; Di Iorio, D.; Bowen, A.; Reddy, C. M.; Techet, A. H.; Yoerger, D. R.; Whitcomb, L. L.; Seewald, J. S.; Sylva, S. P.; Fenwick, J. Acoustic Measurement of the Deepwater Horizon Macondo Well Flow Rate. *Proceedings of the National Academy of Sciences* **2011**, *109*, 20235–20239.
2. OSAT Summary report for Sub-Sea and Sub-Surface Oil and Dispersant Detection: Sampling and monitoring, December 17, 2010, [http://www.restorethegulf.gov/sites/default/files/documents/pdf/OSAT\\_Report\\_FINAL\\_17DEC.pdf](http://www.restorethegulf.gov/sites/default/files/documents/pdf/OSAT_Report_FINAL_17DEC.pdf).
3. Whitehead, A.; Dubansky, B.; Bodinier, C.; Garcia, T. I.; Miles, S.; Pilley, C.; Raghunathan, V.; Roach, J. L.; Walker, N.; Walter, R. B.; et al. Genomic and Physiological Footprint of the Deepwater Horizon Oil Spill on Resident Marsh Fishes. *Proceedings of the National Academy of Sciences* **2012**, *109*, 20298–20302.
4. Kujawinski, E. B.; Kido Soule, M. C.; Valentine, D. L.; Boysen, A. K.; Longnecker, K.; Redmond, M. C. Fate of Dispersants Associated with the Deepwater Horizon Oil Spill. *Environmental Science & Technology* **2011**, *45*, 1298–1306.
5. Deepwater Horizon: A Preliminary Bibliography of Published Research and Expert Commentary, <http://www.lib.noaa.gov/researchtools/subjectguides/dwh.html>.
6. Ryerson, T. B.; Camilli, R.; Kessler, J. D.; Kujawinski, E. B.; Reddy, C. M.; Valentine, D. L.; Atlas, E.; Blake, D. R.; de Gouw, J.; Meinardi, S.; et al. Chemical Data Quantify Deepwater Horizon Hydrocarbon Flow Rate and Environmental Distribution. *Proceedings of the National Academy of Sciences* **2012**, *109*, 20246–20253.
7. Lehr B, Bristol S, Possolo A (2010) Oil Budget Calculator Deepwater Horizon, Technical Documentation, A Report to the National Incident Command, November 2010, Available at [http://www.restorethegulf.gov/sites/default/files/documents/pdf/OilBudgetCalc\\_Full\\_HQ-Print\\_111110.pdf](http://www.restorethegulf.gov/sites/default/files/documents/pdf/OilBudgetCalc_Full_HQ-Print_111110.pdf).
8. Schrope, M. Dirty Blizzard Buried Deepwater Horizon Oil. *Nature* **2013**.
9. Salar Amoli, H.; Porgam, A.; Bashiri Sadr, Z.; Mohanazadeh, F. Analysis of Metal Ions in Crude Oil by Reversed-phase High Performance Liquid Chromatography Using Short Column. *Journal of Chromatography A* **2006**, *1118*, 82–84.
10. White, H. K.; Hsing, P.-Y.; Cho, W.; Shank, T. M.; Cordes, E. E.; Quattrini, A. M.; Nelson, R. K.; Camilli, R.; Demopoulos, A. W. J.; German, C. R.; et al. Impact of the Deepwater Horizon Oil Spill on a Deep-water Coral Community in the Gulf of Mexico. *Proceedings of the National Academy of Sciences* **2012**, *109*, 20303–20308.
11. Reddy, C. M.; Arey, J. S.; Seewald, J. S.; Sylva, S. P.; Lemkau, K. L.; Nelson, R. K.; Carmichael, C. A.; McIntyre, C. P.; Fenwick, J.; Ventura, G. T.; et al. Composition and Fate of Gas and Oil Released to the Water Column During the Deepwater Horizon Oil Spill. *Proceedings of the National Academy of Sciences* **2012**, *109*, 20229–20234.

12. Stanford, L. A.; Kim, S.; Klein, G. C.; Smith, D. F.; Rodgers, R. P.; Marshall, A. G. Identification of Water-Soluble Heavy Crude Oil Organic-Acids, Bases, and Neutrals by Electrospray Ionization and Field Desorption Ionization Fourier Transform Ion Cyclotron Resonance Mass Spectrometry. *Environmental Science & Technology* **2007**, *41*, 2696–2702.
13. Scarlett, A. G.; Reinardy, H. C.; Henry, T. B.; West, C. E.; Frank, R. A.; Hewitt, L. M.; Rowland, S. J. Acute Toxicity of Aromatic and Non-aromatic Fractions of Naphthenic Acids Extracted from Oil Sands Process-affected Water to Larval Zebrafish. *Chemosphere* **2013**, *93*, 415–420.
14. Wolfe, DA, Scott, KJ, Clayton, JR, Lunz, J, Payne, JR, and Thompson, TA. 1995. Comparative Toxicities of Polar and Non-polar Organic Fractions from Sediments Affected by the Exxon Valdez Oil Spill in Prince William Sound, Alaska. *Chemistry and Ecology*. **19**: 137 – 156.
15. Peterson, C. H. Long-Term Ecosystem Response to the Exxon Valdez Oil Spill. *Science* **2003**, *302*, 2082–2086.
16. Kokaly, R. F.; Couvillion, B. R.; Holloway, J. M.; Roberts, D. A.; Ustin, S. L.; Peterson, S. H.; Khanna, S.; Piazza, S. C. Spectroscopic Remote Sensing of the Distribution and Persistence of Oil from the Deepwater Horizon Spill in Barataria Bay Marshes. *Remote Sensing of Environment* **2013**, *129*, 210–230.
17. Aeppli, C.; Reddy, C. M.; Nelson, R. K.; Kellermann, M. Y.; Valentine, D. L. Recurrent Oil Sheens at the Deepwater Horizon Disaster Site Fingerprinted with Synthetic Hydrocarbon Drilling Fluids. *Environmental Science & Technology* **2013**, *130717151649002*.
18. Credit: NOAA/Kate Sweeney.
19. Maki, H.; Sasaki, T.; Harayama, S. Photo-oxidation of Biodegraded Crude Oil and Toxicity of the Photo-oxidized Products. *Chemosphere* **2001**, *44*, 1145–1151.
20. Liu, Z.; Liu, J.; Zhu, Q.; Wu, W. The Weathering of Oil after the Deepwater Horizon Oil Spill: Insights from the Chemical Composition of the Oil from the Sea Surface, Salt Marshes and Sediments. *Environmental Research Letters* **2012**, *7*, 035302.
21. Kessler, J. D.; Valentine, D. L.; Redmond, M. C.; Du, M.; Chan, E. W.; Mendes, S. D.; Quiroz, E. W.; Villanueva, C. J.; Shusta, S. S.; Werra, L. M.; et al. A Persistent Oxygen Anomaly Reveals the Fate of Spilled Methane in the Deep Gulf of Mexico. *Science* **2011**, *331*, 312–315.
22. Yvon-Lewis, S. A.; Hu, L.; Kessler, J. Methane Flux to the Atmosphere from the Deepwater Horizon Oil Disaster: Methane Flux from the Deepwater Horizon. *Geophysical Research Letters* **2011**, *38*.

23. Ryerson, T. B.; Aikin, K. C.; Angevine, W. M.; Atlas, E. L.; Blake, D. R.; Brock, C. A.; Fehsenfeld, F. C.; Gao, R.-S.; de Gouw, J. A.; Fahey, D. W.; et al. Atmospheric Emissions from the Deepwater Horizon Spill Constrain Air-water Partitioning, Hydrocarbon Fate, and Leak Rate: Deepwater Horizon Atmospheric Emissions. *Geophysical Research Letters* 2011, 38.
24. Charrié-Duhaut, A.; Lemoine, S.; Adam, P.; Connan, J.; Albrecht, P. Abiotic Oxidation of Petroleum Bitumens Under Natural Conditions. *Organic Geochemistry* 2000, 31, 977–1003.
25. Aeppli, C.; Carmichael, C. A.; Nelson, R. K.; Lemkau, K. L.; Graham, W. M.; Redmond, M. C.; Valentine, D. L.; Reddy, C. M. Oil Weathering after the Deepwater Horizon Disaster Led to the Formation of Oxygenated Residues. *Environmental Science & Technology* 2012, 46, 8799–8807.
26. Kiruri, L. W.; Dellinger, B.; Lomnicki, S. Tar Balls from Deep Water Horizon Oil Spill: Environmentally Persistent Free Radicals (EPFR) Formation During Crude Weathering. *Environmental Science & Technology* 2013, 47, 4220–4226.
27. Dutta, T. K.; Harayama, S. Fate of Crude Oil by the Combination of Photooxidation and Biodegradation. *Environmental Science & Technology* 2000, 34, 1500–1505.
28. Atlas, R. M.; Hazen, T. C. Oil Biodegradation and Bioremediation: A Tale of the Two Worst Spills in U.S. History. *Environmental Science & Technology* 2011, 45, 6709–6715.
29. Plant, N.G, Long, J.W., Dalyander, P.S., Thompson, D.M., and Raabe, E.A., 2013, Application of a hydrodynamic and sediment transport model for guidance of response efforts related to the Deepwater Horizon oil spill in the Northern Gulf of Mexico along the coast of Alabama and Florida: U.S. Geological Survey Open-File Report 2012–1234, 46 p., <http://pubs.usgs.gov/of/2012/1234/>.
30. Hall, G. J.; Frysinger, G. S.; Aeppli, C.; Carmichael, C. A.; Gros, J.; Lemkau, K. L.; Nelson, R. K.; Reddy, C. M. Oxygenated Weathering Products of Deepwater Horizon Oil Come from Surprising Precursors. *Marine Pollution Bulletin* 2013, 75, 140–149.
31. Radović, J. R.; Aeppli, C.; Nelson, R. K.; Jimenez, N.; Reddy, C. M.; Bayona, J. M.; Albaigés, J. Assessment of Photochemical Processes in Marine Oil Spill Fingerprinting. *Mar. Pollut. Bull.* 2013.
32. Noda, I. Two-dimensional Correlation Spectroscopy: Applications in Vibrational and Optical Spectroscopy; John Wiley & Sons: Chichester, West Sussex, England ; Hoboken, NJ, 2004.
33. Fernández-Varela, R.; Andrade, J. M.; Muniategui, S.; Prada, D.; Ramírez-Villalobos, F. The Comparison of Two Heavy Fuel Oils in Composition and Weathering Pattern, Based on IR, GC-FID and GC-MS Analyses: Application to the Prestige Wreckage. *Water Res.* 2009, 43, 1015–1026.

## Appendix:

### A: Pristane/phytane ratios

	Raw Oil	A121	A122	B121	B122
C17	10499310	33537105	33482323	32925511	30112144
Pristane	7038824	23676754	22592490	22158817	19857833
C18	9107142	29300681	29066762	28760335	26410222
phytane	4575721	15749015	14666780	13804402	13312393
Pris/Phy	1.538	1.503	1.540	1.605	1.492

	D121	D122	E121	E122
C17	40485041	36985043	34835796	37965198
Pristane	26863291	24224834	23613002	25630777
C18	35343149	31691186	30687301	34751589
phytane	16751231	15054712	14697223	17102082
Pris/Phy	1.604	1.609	1.607	1.499

Ave. Pris/Phy	1.562
Std. Div.	0.048
Std. Error	0.015

## B: Raw oil incubation extraction data

Initial mass of each samples, the extracted mass after incubation, and the percent mass lost.

	A31	B31	C31	D31	E31				
Mass (g)	0.080	0.080	0.080	0.080	0.080				
Ext. (g)	0.059	0.058	0.059	0.057	0.055				
% Loss	74.1	72.8	73.8	71.6	69.0				
	A61	A62	B61	B62	C61	C62	D61	D62	E61
Mass (g)	0.080	0.080	0.080	0.080	0.080	0.080	0.080	0.080	0.080
Ext. (g)	0.076	0.056	0.058	0.065	0.061	0.057	0.070	0.061	0.055
% Loss	94.8	69.8	72.5	81.3	75.9	70.9	87.0	76.3	69.1
	A91	A92	B91	B92	C91	C92	D91	D92	E91
Mass (g)	0.080	0.080	0.080	0.080	0.080	0.080	0.080	0.080	0.080
Ext. (g)	0.059	0.063	0.071	0.062	0.068	0.067	0.055	0.058	0.055
% Loss	73.1	78.4	89.3	78.0	84.6	84.3	69.0	72.0	69.0
	A121	A122	B121	B122	C121	C122	D121	D122	E121
Mass (g)	0.080	0.080	0.080	0.080	0.080	0.080	0.080	0.080	0.080
Ext. (g)	0.056	0.058	0.063	0.066	0.066	0.067	0.054	0.058	0.062
% Loss	69.9	71.9	79.1	82.0	82.6	83.5	67.1	72.3	78.0
	A151	A152	B151	B152	C151	C152	D151	D152	E151
Mass (g)	0.080	0.080	0.080	0.080	0.080	0.080	0.080	0.080	0.080
Ext. (g)	0.058	0.056	0.067	0.065	0.068	0.067	0.058	0.056	0.058
% Loss	72.1	69.8	83.8	81.4	84.6	84.1	72.9	70.1	72.9
	A211	A212	B211	B212	C211	C212	D211	D212	E211
Mass (g)	0.080	0.080	0.080	0.080	0.080	0.080	0.080	0.080	0.080
Ext. (g)	0.064	0.012	0.074	0.079	0.067	0.085	0.055	0.034	0.064
% Loss	80.4	14.6	92.0	98.3	83.9	106.6	69.1	42.9	79.8
									2.0

### C: Raw oil and OSP FT-IR average integrations

Integrations follow the scheme: Free OH (3658-3629 cm<sup>-1</sup>), O-H stretch (3740-3115 cm<sup>-1</sup>), asymmetric CH<sub>3</sub>/CH<sub>2</sub> stretch-referred to as C1 (3030-3877 cm<sup>-1</sup>), symmetric CH<sub>3</sub>/CH<sub>2</sub> stretch-referred to as C2 (3877-2822 cm<sup>-1</sup>), C=O stretch (1813-1670 cm<sup>-1</sup>), C=C stretch (1670-1521 cm<sup>-1</sup>), C-O stretch (1064-1006 cm<sup>-1</sup>).

Raw oil and time point 3 raw oil FT-IR integrations

	Raw Oil	A31	B31	C31	D31	E31
OH	0.000	0.000	0.000	0.000	0.000	0.000
Free OH	0.004	0.013	0.042	0.040	0.065	0.072
C-H 1	57.384	46.878	41.138	42.690	41.180	41.743
CH 2	12.329	10.408	9.273	9.597	9.334	9.379
CH total	95.001	77.500	68.584	72.185	68.258	68.168
C=O	0.000	0.215	0.176	0.098	0.207	0.194
C=C	0.501	0.727	0.601	0.601	0.631	0.699
C-O	0.000	0.092	0.050	0.079	0.096	0.094

Time point 6 raw oil FT-IR integrations

	A61	A62	B61	B62	C61	C62
OH	0.000	0.000	0.000	0.000	0.000	0.000
Free OH	0.009	0.186	0.018	0.041	0.025	0.035
C-H 1	40.034	39.064	39.202	40.147	40.703	42.170
CH 2	9.178	8.845	8.946	9.009	9.220	9.447
CH total	67.331	64.834	65.685	67.059	68.209	70.589
C=O	0.382	0.413	0.163	0.094	0.253	0.107
C=C	0.902	0.691	0.760	0.633	0.784	0.524
C-O	0.134	0.410	0.092	0.108	0.105	0.090
	D61	D62	E61	E62		
OH	0.000	0.000	0.000	0.000		
Free OH	0.081	0.074	0.077	0.280		
C-H 1	42.184	40.247	38.462	41.345		
CH 2	9.485	9.083	8.791	9.127		
CH total	70.449	67.065	64.025	68.342		
C=O	0.256	0.295	0.171	0.235		
C=C	0.710	0.585	0.642	0.574		
C-O	0.185	0.167	0.164	0.635		

Time point 9 raw oil FT-IR integrations

	A91	A92	B91	B92	C91	C92
OH	0.000	0.000	0.000	0.000	0.000	0.000
Free OH	0.119	0.570	0.037	0.016	0.139	0.033
C-H 1	29.274	36.730	41.746	40.735	42.145	41.983
CH 2	6.319	8.213	9.241	9.178	9.292	9.171
CH total	48.837	60.948	69.577	67.312	70.162	69.489
C=O	0.173	0.406	0.230	0.288	0.125	0.190
C=C	0.510	0.705	0.653	0.620	0.638	0.596
C-O	0.191	0.077	0.109	0.111	0.309	0.083
	D91	D92	E91	E92		
OH	0.000	0.000	0.000	0.000		
Free OH	0.190	0.035	0.090	0.072		
C-H 1	38.540	39.249	37.419	37.169		
CH 2	8.589	8.800	8.457	8.560		
CH total	64.099	64.531	62.249	62.073		
C=O	0.246	0.505	0.135	0.364		
C=C	0.610	0.661	0.584	0.683		
C-O	0.369	0.071	0.194	0.177		

Time point 12 raw oil FT-IR integrations

	A121	A122	B121	B122	C121	C122
OH	0.000	0.000	0.000	0.000	0.000	0.000
Free OH	0.002	0.012	0.014	0.026	0.015	0.021
C-H 1	45.925	39.225	42.288	39.992	40.806	41.283
CH 2	10.020	9.002	9.528	9.012	9.167	9.277
CH total	77.301	65.506	70.781	66.929	68.214	69.029
C=O	0.387	0.394	0.180	0.147	0.152	0.153
C=C	0.913	0.897	0.733	0.669	0.652	0.640
C-O	0.164	0.150	0.185	0.166	0.162	0.160
	D121	D122	E121	E122		
OH	0.000	0.000	0.000	0.000		
Free OH	0.061	0.112	0.030	0.034		
C-H 1	38.839	39.259	40.349	38.025		
CH 2	8.888	8.972	9.194	8.706		
CH total	64.890	65.556	67.465	63.427		
C=O	0.251	0.276	0.178	0.181		
C=C	0.685	0.710	0.721	0.678		
C-O	0.180	0.164	0.182	0.189		

Time point 15 raw oil FT-IR integrations

	A151	A152	B151	B152	C151	C152
OH	0.000	0.000	0.000	0.000	0.000	0.000
Free OH	0.001	0.075	0.061	0.024	0.058	0.041
C-H 1	39.702	36.502	42.695	42.392	43.444	42.489
CH 2	9.004	8.392	9.516	9.557	9.682	9.537
CH total	66.695	61.031	71.625	71.046	72.620	71.053
C=O	0.394	0.341	0.150	0.175	0.157	0.153
C=C	0.852	0.780	0.678	0.694	0.651	0.650
C-O	0.082	0.104	0.109	0.083	0.088	0.099
	D151	D152	E151	E152		
OH	0.000	0.000	0.000	0.000		
Free OH	0.032	0.006	0.085	0.026		
C-H 1	40.234	40.804	36.382	38.885		
CH 2	9.161	9.402	8.474	8.978		
CH total	67.143	68.508	60.895	65.307		
C=O	0.305	0.325	0.242	0.219		
C=C	0.712	0.849	0.758	0.759		
C-O	0.085	0.114	0.186	0.146		

Time point 21 raw oil FT-IR integrations

	A211	A212	B211	B212	C211	C212
OH	0.000	0.000	0.000	0.000	0.000	0.000
Free OH	0.043	0.046	0.104	0.080	0.038	0.015
C-H 1	27.269	31.776	30.216	22.881	29.146	21.557
CH 2	6.516	7.189	6.736	5.546	6.568	5.391
CH total	43.375	51.788	49.517	36.642	47.637	34.143
C=O	0.476	0.376	0.167	0.179	0.160	0.073
C=C	0.767	0.686	0.665	0.551	0.451	0.487
C-O	0.095	0.152	0.286	0.223	0.133	0.034
	D211	D212	E211	E212		
OH	0.000	0.000	0.000	0.000		
Free OH	0.112	0.060	0.220	0.006		
C-H 1	28.218	31.857	24.992	24.508		
CH 2	6.587	7.202	6.183	5.342		
CH total	45.679	51.990	39.474	34.781		
C=O	0.292	0.290	0.239	0.246		
C=C	0.710	0.614	0.718	0.718		
C-O	0.311	0.175	0.524	0.085		

### Raw Oil and initial OSP FT-IR integrations

	Raw Oil	T0_SP2	T0_EI28_A
OH	0.000	12.044	12.650
Free OH	0.004	0.173	0.174
C-H 1	57.384	94.554	43.629
CH 2	12.329	19.544	9.001
CH total	95.001	150.016	77.641
C=O	0.000	3.952	2.120
C=C	0.501	3.779	4.217
C-O	0.000	0.435	0.717

### OSP time point 3 FT-IR integrations

	T3_SP2_A	T3_SP2_B	T3_SP2_C	T3_SP2_D
OH	10.388	29.623	9.446	15.209
Free OH	0.501	0.033	0.128	0.572
C-H 1	29.131	23.035	34.802	31.827
CH 2	6.303	4.572	7.648	6.763
CH total	47.426	33.742	59.084	53.126
C=O	2.270	3.500	2.104	3.407
C=C	5.751	5.553	5.376	4.996
C-O	1.633	0.277	0.253	1.948
	T3_EI28_A	T3_EI28_B	T3_EI28_C	T3_EI28_D
OH	7.519	11.717	7.981	10.126
Free OH	0.183	0.084	0.223	0.111
C-H 1	27.965	23.680	39.256	24.731
CH 2	5.793	4.783	8.012	4.966
CH total	46.272	38.578	68.841	41.881
C=O	2.115	2.114	2.433	2.592
C=C	4.589	4.494	4.800	5.558
C-O	0.709	0.440	0.272	0.329

OSP time point 6 FT-IR integrations

	T6_SP2_A	T6_SP2_B	T6_SP2_C	T6_SP2_D
OH	8.520	13.896	10.669	24.998
Free OH	0.092	0.118	0.147	0.322
C-H 1	23.350	24.711	28.589	77.788
CH 2	5.101	5.427	6.682	16.652
CH total	33.745	36.035	45.973	133.712
C=O	1.290	1.630	2.071	4.171
C=C	4.367	4.490	6.361	10.700
C-O	0.258	0.230	0.429	1.936
	T6_EI28_A	T6_EI28_B	T6_EI28_C	T6_EI28_D
OH	10.932	17.348	8.306	21.002
Free OH	0.180	0.249	0.177	0.881
C-H 1	23.505	23.611	22.127	25.159
CH 2	4.912	5.130	4.805	5.433
CH total	38.172	39.290	33.293	38.278
C=O	1.884	1.540	1.306	1.900
C=C	5.367	4.101	3.734	5.204
C-O	0.866	1.861	1.130	2.732

## D: Raw oil and OSP FT-IR average peak ratios

Total ratios from raw oil time series A (light, abiotic)

	A3	A6	A9	A12	A15	A21
C-H1:C-H2	4.504	4.389	4.552	4.470	4.379	4.303
CH total:C-H1	1.653	1.671	1.664	1.677	1.676	1.610
CH total:C-H2	7.446	7.333	7.575	7.496	7.340	6.930
Free OH:C-H1	0.000	0.002	0.010	0.000	0.001	0.002
Free OH:C-H2	0.001	0.011	0.044	0.001	0.005	0.006
Free OH:CH total	0.000	0.002	0.006	0.000	0.001	0.001
C=O:C-H1	0.005	0.010	0.008	0.009	0.010	0.015
C=O:C-H2	0.021	0.044	0.038	0.041	0.042	0.063
C=O:CH total	0.003	0.006	0.005	0.006	0.006	0.009
C=C:C-H1	0.016	0.020	0.018	0.021	0.021	0.025
C=C:C-H2	0.070	0.088	0.083	0.095	0.094	0.107
C=C:Ch total	0.009	0.012	0.011	0.013	0.013	0.015
O-H:C-H1	0.002	0.007	0.004	0.004	0.002	0.004
O-H:C-H2	0.009	0.030	0.020	0.017	0.011	0.018
O-H:CH total	0.001	0.004	0.003	0.002	0.001	0.003
Free OH:C=O	0.060	0.237	1.045	0.018	0.111	0.106
C=O:C=C	0.296	0.511	0.458	0.432	0.450	0.584
C=O:O-H	2.337	1.929	3.089	2.493	4.042	3.742

Total ratios from raw oil time series B (dark, biotic)

	B3	B6	B9	B12	B15	B21
C-H1:C-H2	4.436	4.419	4.478	4.438	4.461	4.306
CH total:C-H1	1.667	1.673	1.660	1.674	1.677	1.620
CH total:C-H2	7.396	7.393	7.432	7.428	7.480	6.979
Free OH:C-H1	0.001	0.001	0.001	0.000	0.001	0.003
Free OH:C-H2	0.005	0.003	0.003	0.002	0.004	0.015
Free OH:CH total	0.001	0.000	0.000	0.000	0.001	0.002
C=O:C-H1	0.004	0.003	0.006	0.004	0.004	0.007
C=O:C-H2	0.019	0.014	0.028	0.018	0.017	0.028
C=O:CH total	0.003	0.002	0.004	0.002	0.002	0.004
C=C:C-H1	0.015	0.018	0.015	0.017	0.016	0.023
C=C:C-H2	0.065	0.078	0.069	0.076	0.072	0.099
C=C:Ch total	0.009	0.011	0.009	0.010	0.010	0.010
O-H:C-H1	0.001	0.003	0.003	0.004	0.002	0.010
O-H:C-H2	0.005	0.011	0.012	0.019	0.010	0.041
O-H:CH total	0.001	0.002	0.002	0.003	0.001	0.006
Free OH:C=O	0.239	0.273	0.108	0.127	0.272	0.535
C=O:C=C	0.293	0.181	0.408	0.233	0.237	0.288
C=O:O-H	3.520	1.321	2.352	0.929	1.742	0.692

Total ratios from raw oil time series C (dark, abiotic)

	C3	C6	C9	C12	C15	C21
C-H1:C-H2	4.448	4.439	4.557	4.451	4.471	4.218
CH total:C-H1	1.691	1.675	1.660	1.672	1.672	1.609
CH total:C-H2	7.522	7.435	7.564	7.441	7.475	6.793
Free OH:C-H1	0.001	0.001	0.002	0.000	0.001	0.001
Free OH:C-H2	0.004	0.003	0.009	0.002	0.005	0.004
Free OH:CH total	0.001	0.000	0.001	0.000	0.001	0.001
C=O:C-H1	0.002	0.004	0.004	0.004	0.004	0.004
C=O:C-H2	0.010	0.019	0.017	0.017	0.016	0.019
C=O:CH total	0.001	0.003	0.002	0.002	0.002	0.003
C=C:C-H1	0.014	0.016	0.015	0.016	0.015	0.019
C=C:C-H2	0.063	0.070	0.067	0.070	0.068	0.080
C=C:Ch total	0.008	0.009	0.009	0.009	0.009	0.010
O-H:C-H1	0.002	0.002	0.005	0.004	0.002	0.003
O-H:C-H2	0.008	0.010	0.021	0.017	0.010	0.013
O-H:CH total	0.001	0.001	0.003	0.002	0.001	0.002
Free OH:C=O	0.408	0.213	0.643	0.118	0.319	0.221
C=O:C=C	0.163	0.263	0.257	0.236	0.238	0.252
C=O:O-H	1.241	1.799	1.347	0.947	1.665	1.675

Total ratios from raw oil time series D (light, biotic)

	D3	D6	D9	D12	D15	D21
C-H1:C-H2	4.412	4.439	4.474	4.373	4.366	4.354
CH total:C-H1	1.658	1.668	1.654	1.670	1.674	1.625
CH total:C-H2	7.313	7.405	7.398	7.304	7.308	7.077
Free OH:C-H1	0.002	0.002	0.003	0.002	0.000	0.003
Free OH:C-H2	0.007	0.008	0.013	0.010	0.002	0.013
Free OH:CH total	0.001	0.001	0.002	0.001	0.000	0.002
C=O:C-H1	0.005	0.007	0.010	0.007	0.008	0.010
C=O:C-H2	0.022	0.030	0.043	0.030	0.034	0.042
C=O:CH total	0.003	0.004	0.006	0.004	0.005	0.006
C=C:C-H1	0.015	0.016	0.016	0.018	0.019	0.022
C=C:C-H2	0.068	0.070	0.073	0.078	0.084	0.097
C=C:Ch total	0.009	0.009	0.010	0.011	0.011	0.014
O-H:C-H1	0.002	0.004	0.006	0.004	0.002	0.008
O-H:C-H2	0.010	0.019	0.026	0.019	0.011	0.036
O-H:CH total	0.001	0.003	0.003	0.003	0.001	0.005
Free OH:C=O	0.314	0.283	0.421	0.324	0.062	0.295
C=O:C=C	0.328	0.432	0.584	0.378	0.406	0.442
C=O:O-H	2.156	1.575	3.890	1.539	3.220	1.298

Total ratios from time series E (dark, elevated temp)

	E3	E6	E9	E12	E15	E21
C-H1:C-H2	4.451	4.453	4.383	4.378	4.312	4.315
CH total:C-H1	1.633	1.659	1.667	1.670	1.677	1.499
CH total:C-H2	7.268	7.385	7.306	7.312	7.230	6.448
	0.002	0.004	0.002	0.001	0.002	0.005
Free OH:C-H2	0.008	0.020	0.010	0.004	0.006	0.018
Free OH:CH total	0.001	0.003	0.001	0.000	0.001	0.003
C=O:C-H1	0.005	0.005	0.007	0.005	0.006	0.010
C=O:C-H2	0.021	0.023	0.029	0.020	0.026	0.042
C=O:CH total	0.003	0.003	0.004	0.003	0.004	0.007
C=C:C-H1	0.017	0.015	0.017	0.018	0.020	0.029
C=C:C-H2	0.075	0.068	0.074	0.078	0.087	0.125
C=C:Ch total	0.010	0.009	0.010	0.011	0.012	0.019
O-H:C-H1	0.002	0.010	0.005	0.005	0.004	0.012
O-H:C-H2	0.010	0.044	0.022	0.021	0.019	0.050
O-H:CH total	0.001	0.006	0.003	0.003	0.003	0.008
Free OH:C=O	0.371	0.821	0.432	0.178	0.235	0.473
C=O:C=C	0.278	0.338	0.382	0.257	0.304	0.338
C=O:O-H	2.064	0.706	1.376	0.968	1.401	1.673

Total ratios from OSP time series A (light, abiotic)

	T0_SP2_A	T3_SP2_A	T6_SP2_A	T0_EI28_A	T3_EI28_A	T6_EI28_A
C-H1:C-H2	4.838	4.622	4.578	4.847	4.827	4.785
CH total:C-H1	1.587	1.628	1.445	1.780	1.655	1.624
CH total:C-H2	7.676	7.524	6.615	8.626	7.988	7.771
Free OH:C-H1	0.002	0.017	0.004	0.004	0.007	0.008
Free OH:C-H2	0.009	0.079	0.018	0.019	0.032	0.037
Free OH:CH total	0.001	0.011	0.003	0.002	0.004	0.005
C=O:C-H1	0.042	0.078	0.055	0.049	0.076	0.080
C=O:C-H2	0.202	0.360	0.253	0.236	0.365	0.384
C=O:CH total	0.026	0.048	0.038	0.027	0.046	0.049
C=C:C-H1	0.040	0.197	0.187	0.097	0.164	0.228
C=C:C-H2	0.193	0.912	0.856	0.469	0.792	1.093
C=C:Ch total	0.025	0.121	0.129	0.054	0.099	0.141
O-H:C-H1	0.005	0.056	0.011	0.016	0.025	0.037
O-H:C-H2	0.022	0.259	0.051	0.080	0.122	0.176
O-H:CH total	0.003	0.034	0.008	0.009	0.015	0.023
Free OH:C=O	0.044	0.220	0.071	0.082	0.087	0.095
C=O:C=C	1.046	0.395	0.295	0.503	0.461	0.351
C=O:O-H	9.085	1.390	5.000	2.957	2.983	2.176

Total ratios from OSP time series B (dark, biotic)

	T0_SP2_B	T3_SP2_B	T6_SP2_B	T0_EI28_B	T3_EI28_B	T6_EI28_B
C-H1:C-H2	4.838	5.038	4.553	4.847	4.951	4.603
CH total:C-H1	1.587	1.465	1.458	1.780	1.629	1.664
CH total:C-H2	7.676	7.380	6.640	8.626	8.066	7.659
Free OH:C-H1	0.002	0.001	0.005	0.004	0.004	0.011
Free OH:C-H2	0.009	0.007	0.022	0.019	0.017	0.049
Free OH:CH total	0.001	0.001	0.003	0.002	0.002	0.006
C=O:C-H1	0.042	0.152	0.066	0.049	0.089	0.065
C=O:C-H2	0.202	0.766	0.300	0.236	0.442	0.300
C=O:CH total	0.026	0.104	0.045	0.027	0.055	0.039
C=C:C-H1	0.040	0.241	0.182	0.097	0.190	0.174
C=C:C-H2	0.193	1.215	0.827	0.469	0.940	0.799
C=C:Ch total	0.025	0.165	0.125	0.054	0.116	0.104
O-H:C-H1	0.005	0.012	0.009	0.016	0.019	0.079
O-H:C-H2	0.022	0.061	0.042	0.080	0.092	0.363
O-H:CH total	0.003	0.008	0.006	0.009	0.011	0.047
Free OH:C=O	0.044	0.009	0.072	0.082	0.040	0.162
C=O:C=C	1.046	0.630	0.363	0.503	0.470	0.376
C=O:O-H	9.085	12.635	7.087	2.957	4.805	0.828

Total ratios from OSP time series C (dark, abiotic)

	T0_SP2_C	T3_SP2_C	T6_SP2_C	T0_EI28_C	T3_EI28_C	T6_EI28_C
C-H1:C-H2	4.838	4.550	4.279	4.847	4.900	4.605
CH total:C-H1	1.587	1.698	1.608	1.780	1.754	1.505
CH total:C-H2	7.676	7.725	6.880	8.626	8.592	6.929
Free OH:C-H1	0.002	0.004	0.005	0.004	0.006	0.008
Free OH:C-H2	0.009	0.017	0.022	0.019	0.028	0.037
Free OH:CH total	0.001	0.002	0.003	0.002	0.003	0.005
C=O:C-H1	0.042	0.060	0.072	0.049	0.062	0.059
C=O:C-H2	0.202	0.275	0.310	0.236	0.304	0.272
C=O:CH total	0.026	0.036	0.045	0.027	0.035	0.039
C=C:C-H1	0.040	0.154	0.222	0.097	0.122	0.169
C=C:C-H2	0.193	0.703	0.952	0.469	0.599	0.777
C=C:Ch total	0.025	0.091	0.138	0.054	0.070	0.112
O-H:C-H1	0.005	0.007	0.015	0.016	0.007	0.051
O-H:C-H2	0.022	0.033	0.064	0.080	0.034	0.235
O-H:CH total	0.003	0.004	0.009	0.009	0.004	0.034
Free OH:C=O	0.044	0.061	0.071	0.082	0.092	0.136
C=O:C=C	1.046	0.391	0.326	0.503	0.507	0.350
C=O:O-H	9.085	8.316	4.828	2.957	8.945	1.156

Total ratios from OSP time series D (light, biotic)

	T0_SP2_D	T3_SP2_D	T6_SP2_D	T0_EI28_D	T3_EI28_D	T6_EI28_D
C-H1:C-H2	4.838	4.706	4.671	4.847	4.980	4.631
CH total:C-H1	1.587	1.669	1.719	1.780	1.693	1.521
CH total:C-H2	7.676	7.855	8.030	8.626	8.434	7.045
Free OH:C-H1	0.002	0.018	0.004	0.004	0.004	0.035
Free OH:C-H2	0.009	0.085	0.019	0.019	0.022	0.162
Free OH:CH total	0.001	0.011	0.002	0.002	0.003	0.023
C=O:C-H1	0.042	0.107	0.054	0.049	0.105	0.076
C=O:C-H2	0.202	0.504	0.250	0.236	0.522	0.350
C=O:CH total	0.026	0.064	0.031	0.027	0.062	0.050
C=C:C-H1	0.040	0.157	0.138	0.097	0.225	0.207
C=C:C-H2	0.193	0.739	0.643	0.469	1.119	0.958
C=C:Ch total	0.025	0.094	0.080	0.054	0.133	0.136
O-H:C-H1	0.005	0.061	0.025	0.016	0.013	0.109
O-H:C-H2	0.022	0.288	0.116	0.080	0.066	0.503
O-H:CH total	0.003	0.037	0.014	0.009	0.008	0.071
Free OH:C=O	0.044	0.168	0.077	0.082	0.043	0.464
C=O:C=C	1.046	0.682	0.390	0.503	0.466	0.365
C=O:O-H	9.085	1.749	2.154	2.957	7.878	0.695